People's Democratic Republic Of Algeria

Ministry Of Higher Education Scientific And Research

University Of Djillali BOUNAAMA - Khemis Miliana

Faculty Of Science And Technology

Department of Electrical Engineering

End-of-study project dissertation with the view of obtaining the degree

Option: INDUSTRIAL ELECTRICAL ENGINEERING

Theme:

Realization of maximum power tracker for photovoltaic system

Prepared By: Mr.Munyaradzi Tigere

Supervisor: Dr.M.Kaci

Jury:

Dr.Z. Layate (president)

Pr.M. Matallah (examiner)

2022/2023

Acknowledgements

First of all, I thank the almighty God for giving me the health, the courage, the will and the patience to complete this work in the best conditions.

I would like to thank professor Meziane Kaci for his guidance, assistance and patience. I'd also like to thank my parents for their help in allowing me to focus on my studies and research. furthermore, I would want to thank my classmates for their generous assistance.

I would also like to thank all the professors of electrical engineering department of Djillali Bounaama University.

Dedication

Thanks to the almighty God, I have completed the realization of this work which I would like to dedicate to:

- ***my parents, my brothers and my sisters.***

- ***My friends Sara Hamzaoui, Tanyaradzwa Murapa and Lisa Yevai Mugariri.***

- ***all my classmates who have always helped and supported me.***

Abstract

The real-world implementation of maximum power point tracking (MPPT) controllers for photovoltaic (PV) systems remains a significant issue for researchers working in this field. Before implementing their MPPT algorithms, they frequently employ simulation tools to evaluate their performance. In this regard, the purpose of this work is to offer a reliable simulation of a PV system constructed using Proteus software. The proposed PV simulator can be used to verify and assess the performance of MPPT algorithms with a closer approximation to the real implementation. The key advantage of this model is that it has a real microcontroller, as can be found in reality, so that the same code for the MPPT algorithm used in simulation will be used in real implementation. In this work, P&O algorithm is presented. The goal is to obtain maximum power using dc dc boost converter.

Keywords: boost converter ; perturbation and observation(P&O) ; MPPT algorithm; PV System.

Résumé

La mise en œuvre dans le monde réel des contrôleurs de suivi du point de puissance maximale (MPPT) pour les systèmes photovoltaïques (PV) reste un problème important pour les chercheurs travaillant dans ce domaine. Avant de mettre en œuvre leurs algorithmes MPPT, ils utilisent fréquemment des outils de simulation pour évaluer leurs performances. À cet égard, le but de ce travail est d'offrir une simulation fiable d'un système PV construit à l'aide du logiciel Proteus. Le simulateur PV proposé peut être utilisé pour vérifier et évaluer les performances des algorithmes MPPT avec une approximation plus proche de la mise en œuvre réelle. L'avantage clé de ce modèle est qu'il dispose d'un véritable microcontrôleur, comme on peut en trouver dans la réalité, de sorte que le même code pour l'algorithme MPPT utilisé en simulation sera utilisé dans l'implémentation réelle. Dans ce travail, l'algorithme P&O est présenté. L'objectif est d'obtenir une puissance maximale en utilisant un convertisseur dc dc boost.

Mots-clés : convertisseur boost ; perturbation et observation(P&O) ; Algorithme MPPT ; Système photovoltaïque.

Table of contents

List of figures

Abbreviations

PV:	photovoltaic
MPPT:	maximum power point tracking
P&O:	perturbation and observation
INC:	incremental conductance
DC:	direct current
PWM:	Pulse Width Modulation
MOSFET:	Metal Oxide Semiconductor Field Effect Transistor
LCD:	Liquid Crystal Display
ASCII:	American Standard Code for Information Interchange
MPP:	maximum power point
LMPP:	local maximum power point
GMMP:	global maximum power point

Nomenclatures

I_{ph}:	photo-current
I_d:	diode current
I_{pv}:	photovoltaic current
V_{pv}:	photovoltaic voltage
V_t:	thermal voltage
V_d:	voltage of diode
T:	absolute temperature in K
T_c:	cell temperature

I_0 : diode saturation current

I_{sh}: shunt current

R_s: series resistance

R_p: shunt resistance

N_p: number of parallel cells in a solar panel

q: electron charge

k: the constant of Boltzmann

V_{oc}: open circuit voltage

I_{sc}: short circuit current

N_s: number of cells in series in photovoltaic panel

a: diode ideality factor of the solar cell

D: duty cycle

General introduction

General introduction

Because of the widespread usage of fossil fuels, pollution of the environment is also a big issue today. Renewable energy technologies have the ability to meet global energy demand while reducing pollution and saving the environment. It is well recognized that among renewable energy sources, solar energy is the most promising and reliable. There are various thermodynamics processes for converting solar energy into energy forms acceptable for human purposes. In general, solar energy conversion can provide heat, kinetic energy, electric energy, and chemical energy[1].

The output characteristics of a PV module are heavily dependent on the solar radiation reaching the PV module's active surface and the PV module's cell temperature. Furthermore, these characteristics have a changeable character based on latitude, solar field direction, season, and hour of day. In other words, the properties of PV panels are determined by the parameters that change throughout the day. These characteristics, notably the power, admit a point corresponding to the maximum power, i.e. the optimum operating point, which is indicated by the abbreviation MPP (maximum power point). A converter is used to continuously locate and track the MPP on the curve PV[2].

This dissertation is organised into four chapters after a general introduction.

The first chapter is focused on Photovoltaic system and their different types. Which explains how photovoltaic cell works and study the influence of irradiance and temperature on a PV module.

The second chapter is devoted to the converters, in particular the boost converter used in this work. Then, it also presents the principle of finding the maximum power point "MPPT" with a few methods, like the incremental conductance algorithm, the perturb and observe method.

In the third chapter, we present the circuit equivalent to the solar cell. After, the simulation of the PV system with the software “Proteus” is presented. After, the simulation of MPPT technique using P&O method is done.

The fourth chapter presents the work of the realization of the boost converter which is controlled by the ARDUINO programmable card. The practical test on PV system by method of the MPPT command: "P&O" is done.

Chapter 1: Photovoltaic system

1.1 Introduction

The low energy conversion efficiency of photovoltaic cells is one of the main issues with using photovoltaic systems, and additionally, during the lengthy operational period of solar cells, their energy conversion efficiency decreases even more due to an increase in operating cell temperature over a certain limit. Maintaining a low operating temperature by cooling a solar system while it is in use is one technique to increase its efficiency[3]. When compared to other sources, energy generation from photovoltaic systems can be generated in an easy manner. As compared to other systems, the number of separate components employed in solar PV systems is quite low[4]. In this chapter, the study of Photovoltaic system and their different types is presented. Next, the working of photovoltaic cell is explained.

1.2 Cells, modules, panel and arrays

The figure 1.1 below shows the cell,module,panel and array.

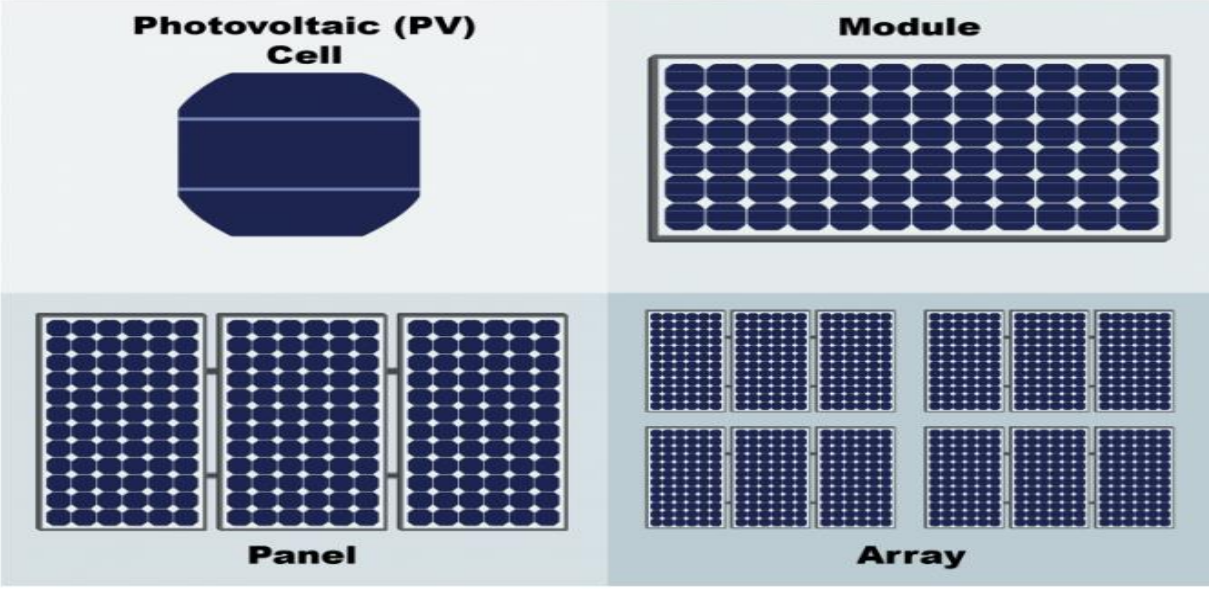

Figure 1.1: cell, panel, module, array.

- A photovoltaic module is a structure in which several solar cells are placed and connected in series or parallel.
- Photovoltaic panels include one or more PV modules assembled as a pre-wired, field-installable unit.
- An array can be created by connecting a number of modules or panels together.

To generate the desired voltage and current, modules can be connected electrically in both parallel and series configurations.

Amorphous silicon, polycrystalline silicon, and monocrystalline silicon are the three types of crystals that can be used to classify silicon-based solar cells.

The figure 1.2 below shows the characteristics of solar cell.

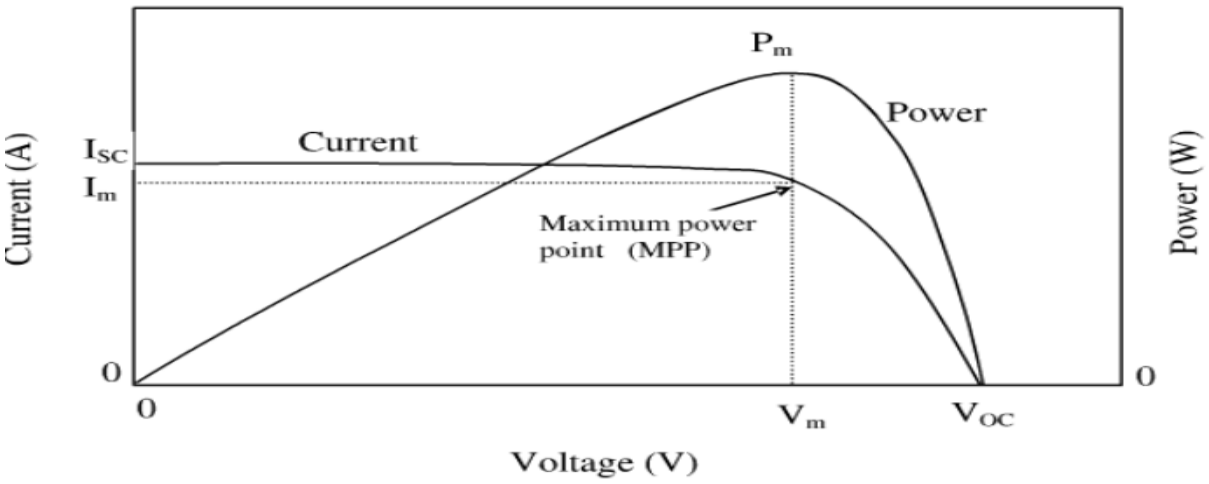

Figure 1.2: IV and PV characteristics of solar panel.

1.3 Solar cells

A solar cell is a type of electrical device that converts light energy directly into electrical energy using the photovoltaic effect. The generation of voltage or current in a material as a result of exposure to sunlight is known as the photovoltaic effect. Without any external voltage source connected, the solar cells can generate electric current[3].

The figure 1.3 below shows the structure of the solar cell.

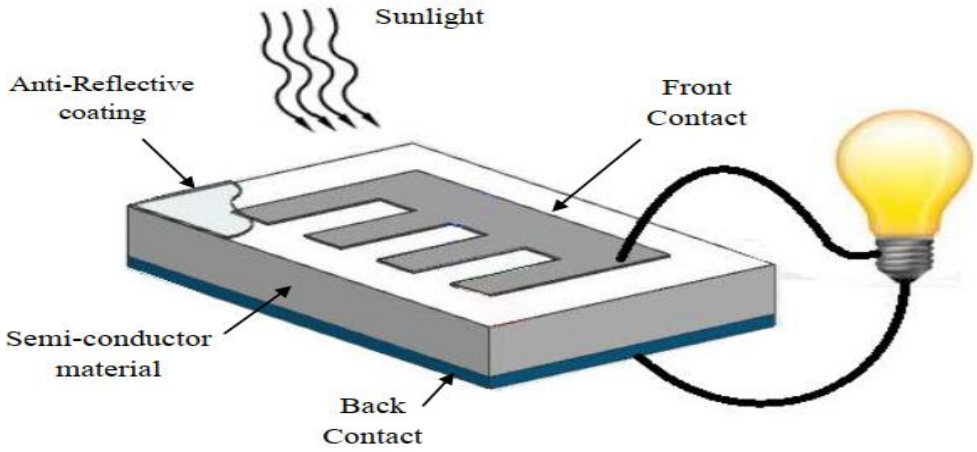

Figure 1.3: solar cell.

1.3.1 Illustration of photovoltaic cell operation.

The most popular semiconductor for PV cells is silicon, a group IV element. There are also other materials that come from a mixture of group III and group V or group II and group VI. GaAs (Gallium Arsenide), GaP (Gallium Phosphide), AlAs (Aluminium Arsenide), AlP (Aluminium Phosphide), and InP are examples of compound semiconductors. Doping is a method that changes the conduction properties of pure semiconductors to create p-type and n-type materials. Combining p-type and n-type semiconductors forms a PV cell.

For instance, (the conduction band is the lowest range of electron energy in which they are free to move, and the valence band is the highest range of electron energy in which they are not). The energy gap for silicon is 1.12 eV. Accordingly, photons with energies of 1.12 eV or above will result in cell current, but photons with energies below 1.12 eV will pass through unabsorbed. A hole forms in the valence band as a result of an electron being lifted from the valence band to the conduction band. The free electrons in the conduction band and holes in the valence band are responsible for the current flow, when the PV cell is connected across a load[5].

1.3.2 Types of solar photovoltaic cells

1.3.2.1 Monocrystalline

Monocrystalline silicon cells are built of pure monocrystalline silicon. The silicon in these cells has a single continuous crystal lattice structure with nearly no flaws or impurities. Monocrystalline cells' main advantage is its high efficiency, which is typically around 15%. The downside of these cells is that they require a complex manufacturing procedure to create monocrystalline silicon, which results in slightly higher costs than those of other technologies. The PV modules have lengthy lifespans thanks to the well-established crystalline silicon cell technology. (20 years or more).

1.3.2.2 Multicrystalline

Multi crystalline silicon is a less expensive material that avoids the costly and energy-intensive crystal formation process. Numerous grains of monocrystalline silicon are used to create multi crystalline cells. Molten Multicrystalline silicon is cast into ingots during the production process, which are then sliced into extremely thin wafers and integrated into whole cells. Due to the less complicated manufacturing method needed, multi crystalline cells are less expensive to create than monocrystalline ones. However, they are marginally less effective, with efficiencies ranging around 12%.

1.3.2.3 Amorphous silicon cells

In general, the main difference between these cells and the ones previously stated above is that amorphous silicon cells are made up of silicon atoms in a thin uniform layer as opposed to having a crystalline structure. Additionally, amorphous silicon, commonly referred to as thin film PV technology, absorbs light more effectively than crystalline silicon, resulting in thinner cells. The fact that amorphous silicon can be placed on a variety of substrates, both rigid and flexible is greatest advantage. Their efficiency is low, ranging about 6%, which is a drawback[6].

The figure 1.4 below shows different types of silicon solar cells.

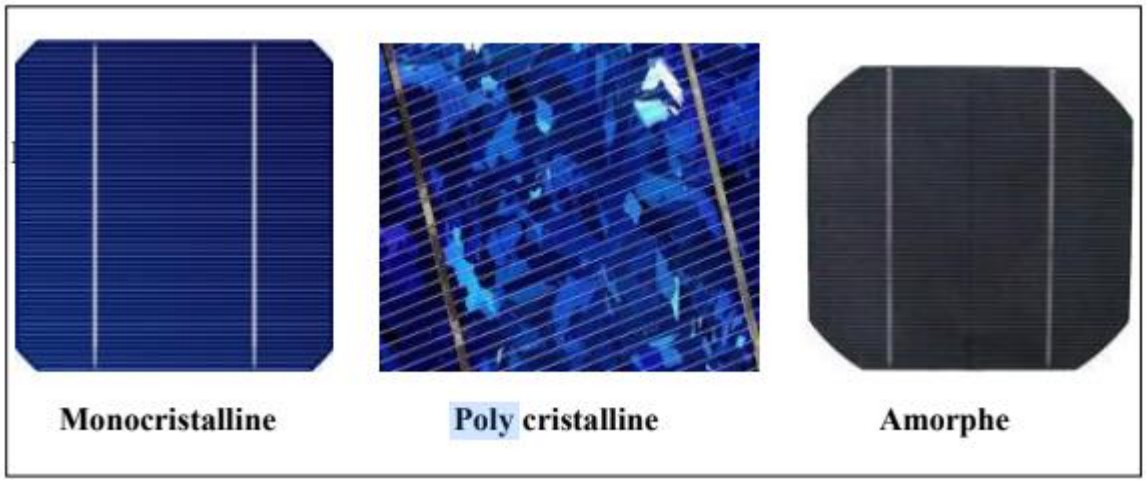

Figure 01.4: monocrystalline, polycrystalline and amorphous solar cells.

1.4 Photovoltaic encapsulation

The need for support and protection of the solar cells is critical given their fragility. A solar cell module typically consists of the support mechanism, the substrate, the superstrate, and the cells themselves coated in an encapsulant. Depending on the substance used, there are various encapsulation techniques, including the most popular one, lamination encapsulation, resin transfer, silicon encapsulation, and vacuum bagging[7]. The encapsulant material adheres firmly to all surfaces, mechanically binding the components into a laminate. The encapsulants should be able to inhibit leakage currents caused by rain or dew wetting by having a high level resistivity to avoid potential induced degradation[8]. Encapsulation is required to shield solar cells from moisture and other outside elements while maintaining electrical and optical transitivity. It also increases the longevity and reliability of the cells[9].

The figure 1.5 below shows the encapsulation of solar cells.

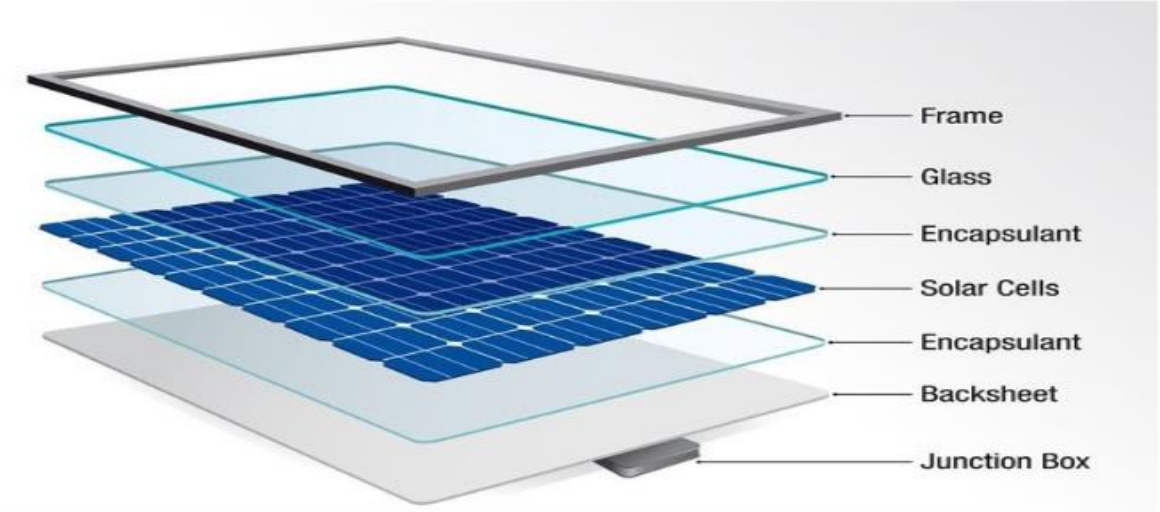

Figure 01.5: Solar cell encapsulation.

1.5 Factors affecting performance of PV Systems

Numerous factors affect a PV module's outdoor performance. Some of these problems are caused by the module itself, while others are because of the environment and location. Among these are solar radiation, module temperature, shading, soiling.

- **Module Temperature**

A PV cell, like any other semiconductor device, is extremely sensitive to temperature. The efficiency and power output of a PV cell decrease as its temperature rises[5]. Every 10 degrees Celsius increase in temperature typically results in a 0.06% decrease in solar cell efficiency[10]. Normalized values of current, voltage, and power at 25oC show that when temperature rises, cell current increases slightly, but voltage falls at a faster rate, resulting in a bigger decline in power output. When the temperature of the cell falls below 25oC, the current decreases somewhat while the voltage and power increase[5]. Aside from temperature, wind direction and wind speed frequency must be considered before picking a site for installation so that air can carry as much heat as possible[10].

Figure 1.6 below shows the effects of temperature on IV characteristics of solar panels.

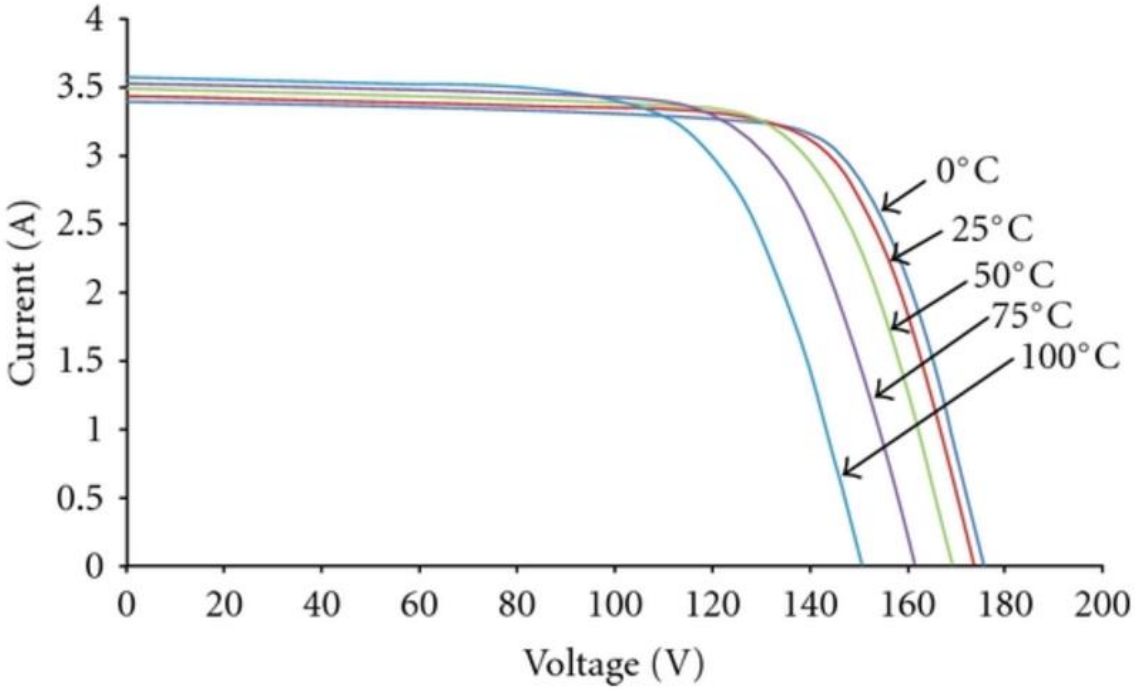

Figure 01.6: IV characteristics of solar panels at different temperatures.

The figure 1.7 shows the effects of temperature on solar panel charecteristics.

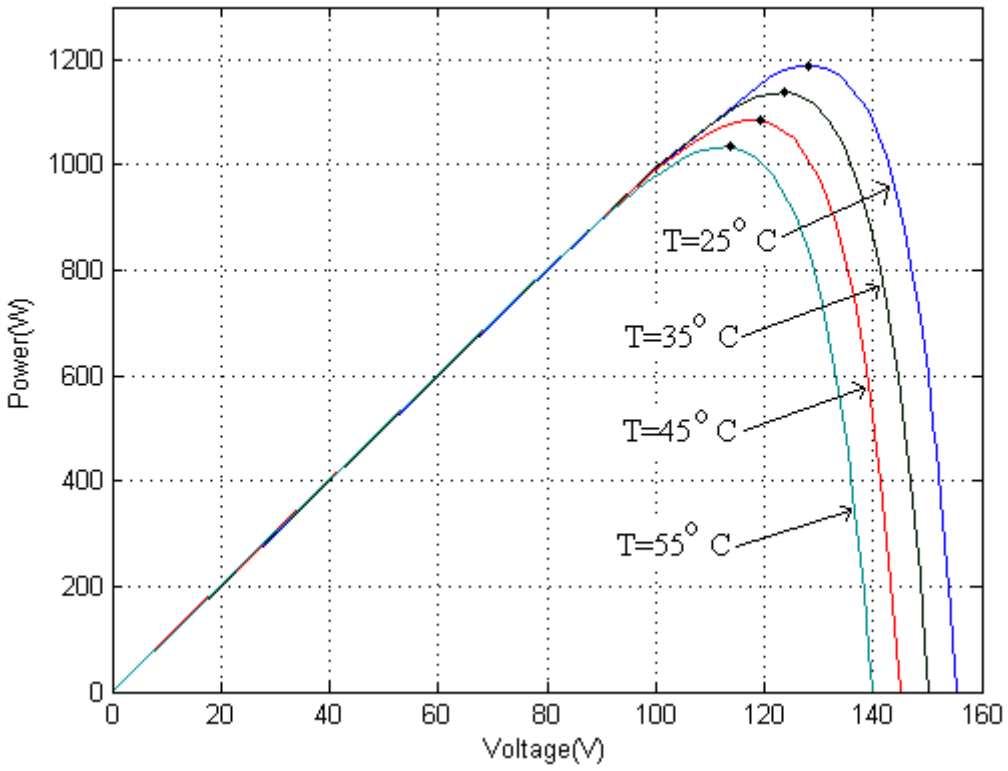

Figure 01.7: PV characteristics of solar panel at different temperatures.

- **Variation in Solar Radiation**

  The change of the spectral irradiance influences the solar power generation[11].

  The figure 1.9 below shows the effects of solar radiation on PV panel caracteristics.

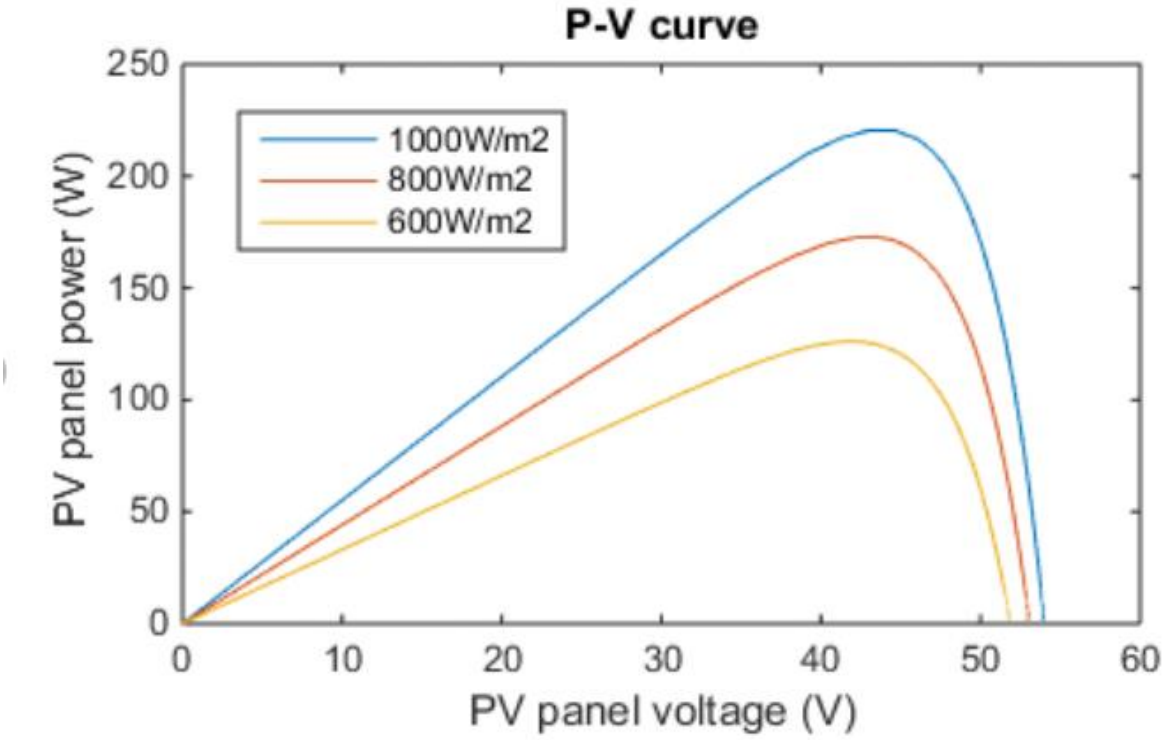

Figure 01.8: effects of radiation on solar panel.

1.6 The different kinds of solar PV system

Grid-tied, hybrid, and off-grid solar PV systems are the three basic types. It actually depends on the customer's goals for their solar panel installation as each form of solar panel system has benefits and drawbacks.

1.6.1 Off-grid solar PV system

A stand-alone power system is an electricity system that is fully off the grid and independent from any electric utility grid. It is utilized in remote locations when alternative energy systems are either not available or are more expensive and complex.

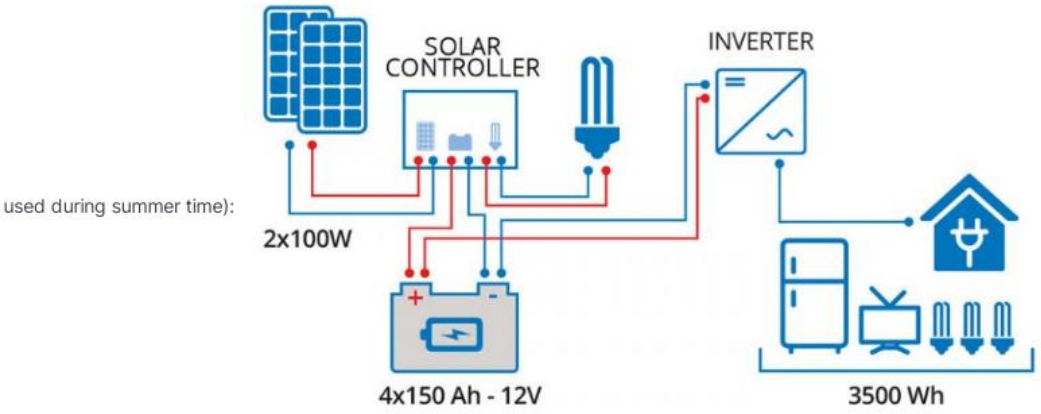

Figure1.9: off-grid PV system.

1.6.2 Grid-tied PV system

Grid-connected generation systems are directly connected to the utility grid; unlike stand-alone photovoltaic power systems, these systems rarely include batteries and they supply the excess power, beyond consumption by the connected load, to the utility grid[12].

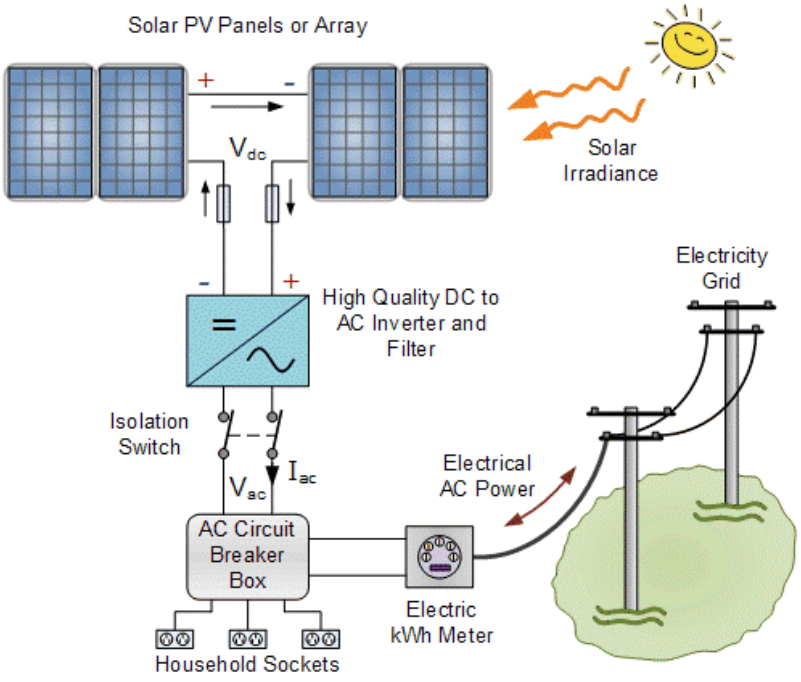

Figure 01.10: grid tied PV system.

1.6.3 Hybrid PV system

The hybrid solar system is net-metered to the grid and has a battery backup to store the power. The energy collected by solar panels is converted into ac electricity by a hybrid solar inverter. The most significant advantage of a hybrid solar system is the power backup capability. It means that even during power outages, you can continue to use electricity without interruption. A battery backup aids in the storage of excess solar electricity generated during peak hours[13].

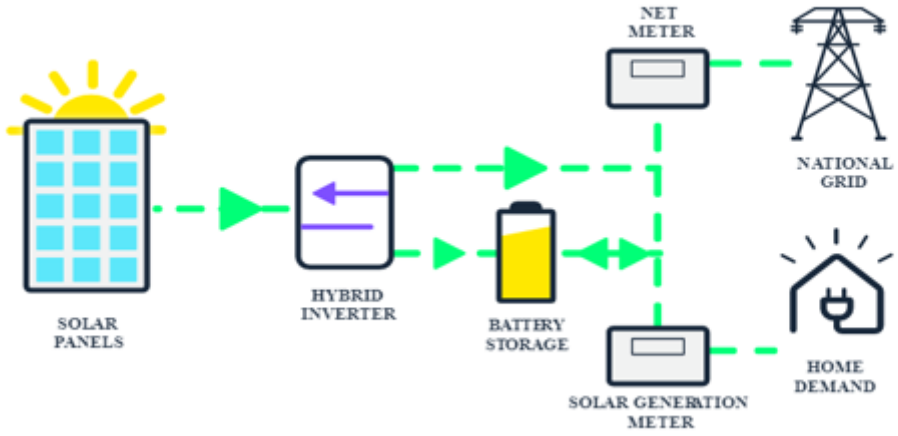

Figure1.11: hybrid PV system.

1.7 Solar PV advantages

1. **A clean and green energy source**

The clean and environmentally friendly energy that PV cells produce is their most notable benefit. There is no concern or fear that the panels will release any dangerous greenhouse gases, such as carbon dioxide, into the atmosphere.

2. **Versatility**

Solar PV cells can generate electricity anywhere. It can be used as a reliable energy source while traveling, camping, and taking lengthy automobile trips because all it needs is sunlight.

3. **Low in maintenance**

Comparing solar PV cells to other renewable energy sources, they are noted for having lower operating and maintenance costs.

4. **Silent**

Solar PV is suitable for urban regions and residential applications because it doesn't make any noise.

5. **Easy to install**

You can easily install residential solar panels on rooftops or just on the ground without interfering with your lifestyle [5].

1.8 Disadvantages

1 The initial cost of purchasing a solar system is high.

2 Weather-Dependent.

3 Solar Energy Storage Is Expensive.

4 Uses a Lot of Space.

5 Associated with Pollution.

1.9 Conclusion

Photovoltaic systems hold immense potential as a sustainable and clean energy source. With the continued deployment of photovoltaic systems and the collective commitment of renewable energy, we can pave the way towards a greener and more sustainable future for generations to come.

In the next chapter, DC/DC converters will be presented as well as the MPPT command.

Chapter 2: DC-DC converters and MPPT techniques

2.1 Introduction

The significance of solar photovoltaic (PV) energy, whose electrical energy is produced by photovoltaic panels, has been growing with the increasing need for electrical energy from nonconventional sources (renewable sources).The photovoltaic system technologies are advancing quickly, playing larger roles in the development of electric power technology, and are recognized as the clean energy[14]. Dc-Dc converters use switching action to change one electrical voltage level into another, making them some of the easiest power electronic circuits. In many places, there is growing interest in these converters. This is because they have so many different uses, including power supplies for computers, workplace equipment, appliances, telecommunications equipment, DC motor drives, automobiles, and airplanes, among others[15].

2.2 DC-DC converters

To receive the DC electricity produced by the solar panel, a converter is connected to the panel's output. A DC-DC converter, also called a DC-DC optimizer, is frequently included. By adjusting the duty cycle of the switching device inside the DC-DC converter, the load characteristics are changed to meet the specifications[16, 17].There are numerous varieties of DC-DC converters. This includes the three types of switching converters (step-down, step-up, and mixed), which are frequently used in photovoltaic systems to produce the desired currents and voltages.

2.2.1 DC-DC boost converter

The voltage of the power output by the DC-DC converter is greater than voltage of the power received with the DC-DC converter.

The figure 2.1 below shows the dc dc boost converter.

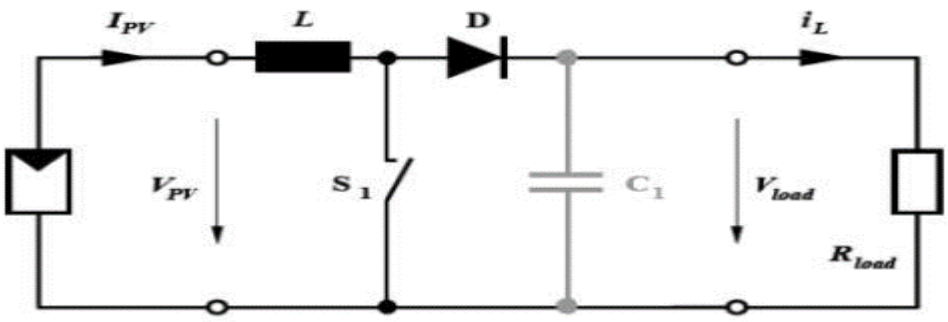

Figure 2.1: boost converter.

The figure below shows the result of switching on and off the DC-DC converter's switch. The switching status of the DC-DC converter switch is shown in the upper graph.
A large value indicates a close switch, while a low value denotes an open switch.
The incoming voltage V_i is less than the output voltage Vo, as shown in the second graph.

The boost converter's inductor current is shown in the third graph.

The following equation, where V_{out} is the output voltage, Vin is the input voltage, and D is the duty cycle, can be used to describe the relationship between the input voltage and output voltage of a boost converter[16].

$$V_{out}=V_{in}/(1-D) \quad (2.1)$$

2.2.1.1 Working of a Boost Converter

The function of boost converter can be divided into two modes, Mode 1 and Mode 2. When transistor S1 is turned on at time t=0, mode 1 begins, Inductor L and transistor S1 conduct the rising incoming current. When transistor S1 is turned off at time t=DT, mode 2 starts. The incoming current is now flowing through L, C, the load, and the diode Dm. The inductor current falls until the next cycle. The energy stored in inductor L flows through the load[18].

The figure 2.2 and figure 2.3 below shows working of the boost converter.

- **Mode 1 (t=0)**

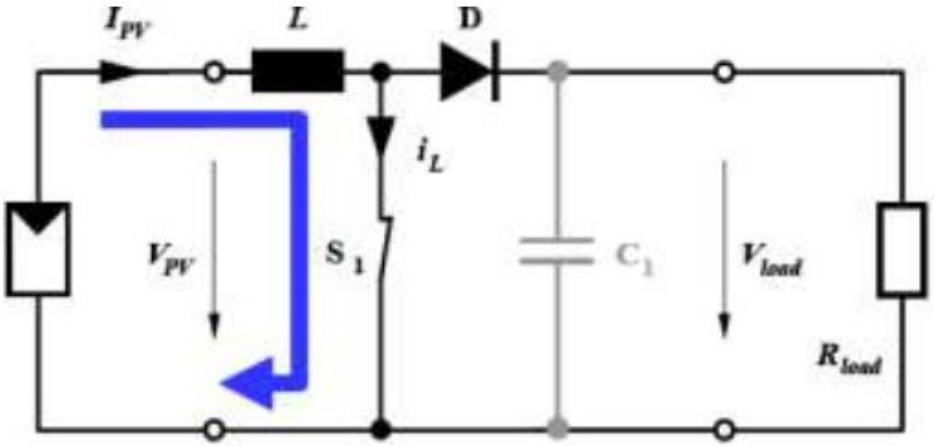

Figure 2.2: closed switch in boost converter.

$$\frac{di_L}{dt}=\frac{V_{in}}{L} \quad (2.2)$$

- **Mode 2 (t=DT)**

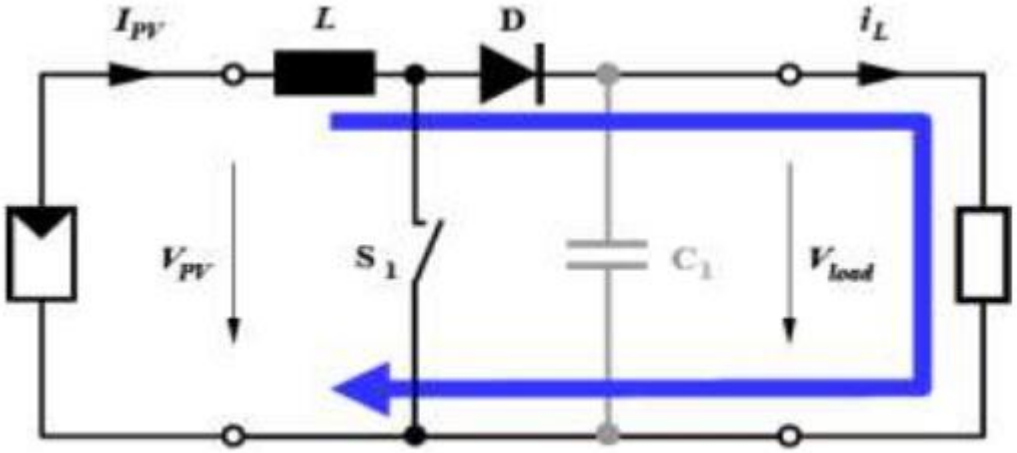

Figure 2.3: open switch in boost converter.

$$\frac{di_L}{dt} = \frac{V_{in} - V_{trans}}{L} \quad (2.3)$$

The boost converter operates in three modes: continuous conduction mode, boundary conduction mode, and discontinuous conduction mode. In continuous conduction state, an inductor's current never falls to zero; it always remains above zero. In a boundary conduction mode, an inductor's current approaches zero for a very short period of time. When the cycle ends or after the cycle ends, the current hits zero. In a discontinuous conduction mode, the inductor current remains zero for a brief time during the cycle; the current reaches zero before the cycle ends and remains zero or less for the rest of the cycle[19].

The figures 2.4, 2.5 and 2.6 shows different modes of conduction of a boost converter.

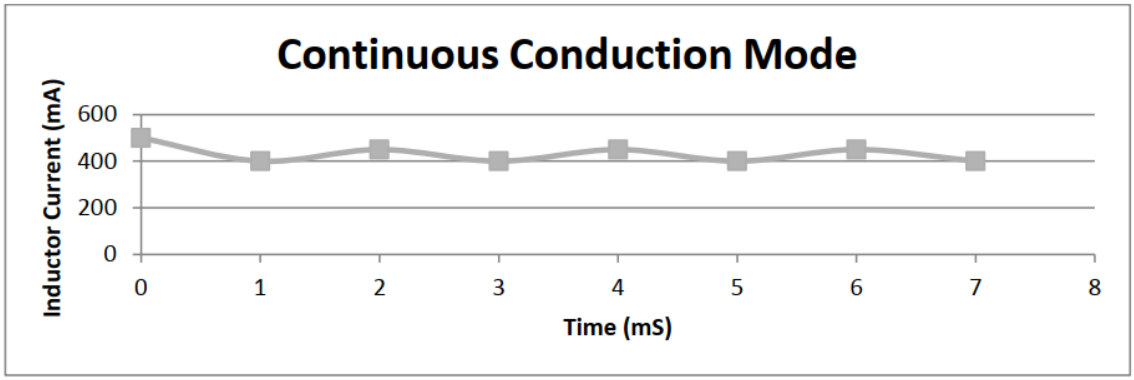

Figure 2,4: continuous conduction mode.

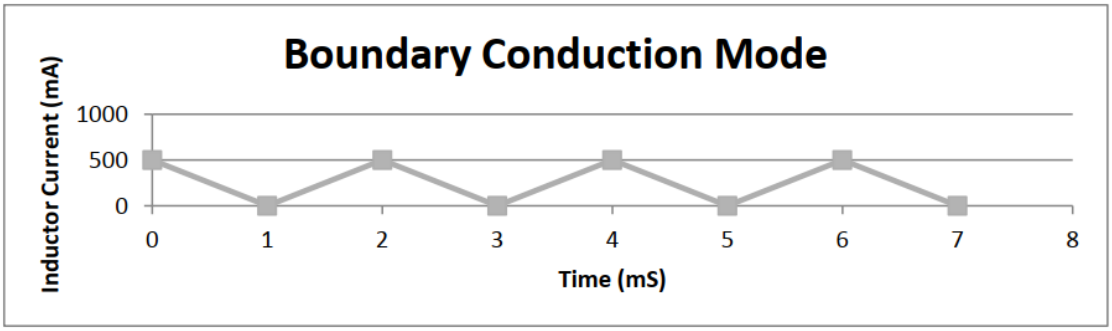

Figure 2.5: boundary conduction mode.

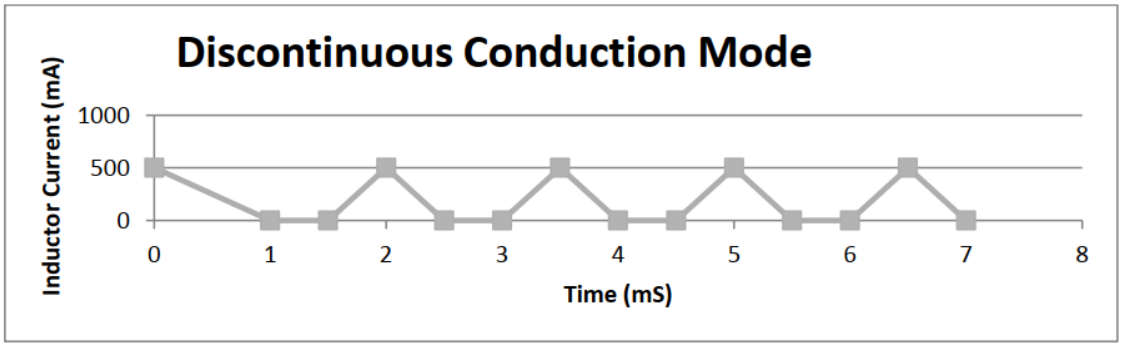

Figure 2.6: discontinuous conduction mode.

2.2.1.2 Derivation of equations

We'll derive the various equations for a boost converter's current and voltage, as well as demonstrate the trade-offs between ripple current and inductance. For the purposes of this dissertation, we will assume that the converter is in continuous mode, which means that the inductor current is never zero.

The waveforms for the voltages and currents for continuous mode are shown in figure below:

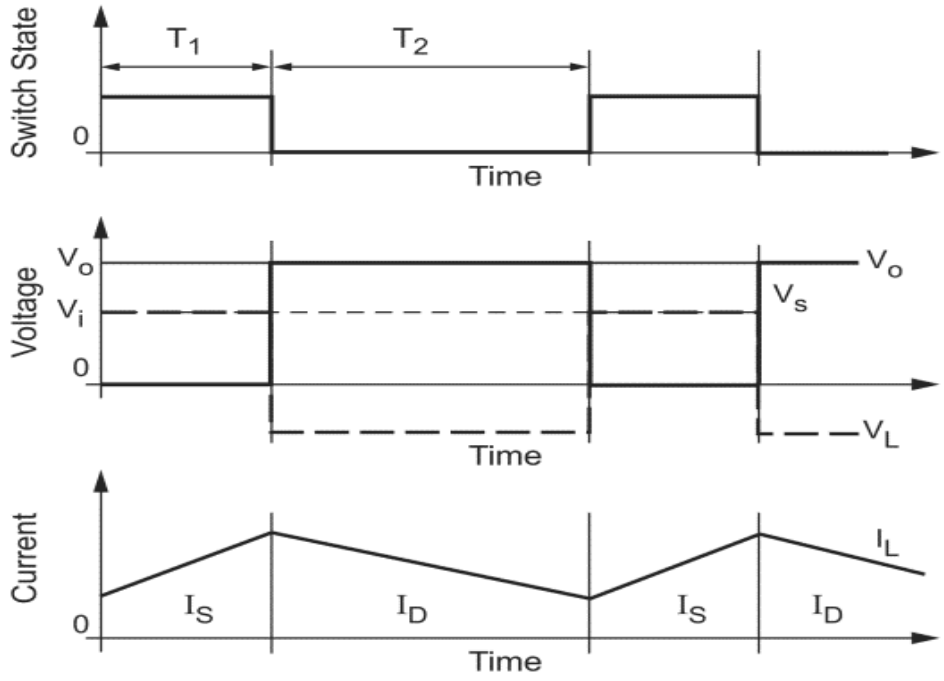

Figure 2.7: current and voltage graphs for a boost converter

The voltage-current relation for the inductor L is:

$$i = \frac{1}{L}\int_0^t V dt + i_0 \tag{2.4}$$

or

$$V = L\frac{di}{dt} \tag{2.5}$$

For a constant rectangular pulse:

$$i = \frac{Vt}{L} + i_0 \tag{2.6}$$

When the transistor is turned on, the current is as follows:

$$i_{pk} = \frac{(V_{in} - V_{trans})T_{on}}{L} + i_0 \tag{2.7}$$

or

$$\Delta i = \frac{(V_{in} - V_{trans})T_{on}}{L} \tag{2.8}$$

When the transistor is turned off, the current is:

$$i_o = i_{pk} - \frac{(V_{out} - V_{in} + V_D)T_{off}}{L} \quad (2.9)$$

or

$$\Delta i = \frac{(V_{out} - V_{in} + V_D)T_{off}}{L} \quad (2.10)$$

Where V_D is the voltage drop across the diode, and V_{Trans} is the voltage drop across the transistor.

By equating through delta i, we can solve for Vout:

$$\frac{(V_{in} - V_{trans})T_{on}}{L} = \frac{(V_{out} - V_{in} + V_D)T_{off}}{L} \quad (2.11)$$

$$V_{in}T_{on} - V_{trans}T_{on} = V_{out}T_{off} - V_{in}T_{off} + V_D T_{off} \quad (2.12)$$

$$V_{in}T_{on} + V_{in}T_{off} = V_{out}T_{off} + V_{trans}T_{on} + V_D T_{off} \quad (2.13)$$

$$V_{in}(T_{on} + T_{off}) = T_{off}(V_{out} + V_D) + V_{trans}T_{on} \quad (2.14)$$

$$V_{in} - V_{trans}D = (V_{out} + V_D)(1 - D) \quad (2.15)$$

$$V_{out} = \frac{(V_{in} - V_{trans}D)}{1 - D} - V_D \quad (2.16)$$

We can also solve for the duty cycle as follows:

$$D = \frac{V_{out} - V_{in} + V_D}{V_{out} + V_D - V_{trans}} \quad (2.17)$$

If we neglect the voltage drops across the transistor and diode, then:

$$V_{out} = \frac{V_{in}}{1 - D} \quad (2.18)$$

So it is clear that the output voltage is related directly to the duty cycle of the pulses. When designing a converter, the primary question is what type of inductor should be used. In most designs, the input voltage, output voltage, and load current are all determined by the design criteria, leaving only inductance and ripple current as free parameters. The inductance is inversely proportionate to the ripple current.

To avoid the instability which is well known for boost converters, and not a problem with buck converters, select an inductor that is large enough for the ripple current to exceed twice the minimal load current. The inductor operates in continuous mode, when this requirement is satisfied.

This can be expressed as follows:

$$L = \frac{(V_{out} - V_{in} + V_D)(1-D)}{i_0 f} \quad (2.19)$$

For higher efficiency the diode should be an ultra-fast recovery diode[20].

2.2.2 The buck-converter

The buck-converter, well known in power electronics, is a circuit used to convert a dc voltage to a lower dc voltage. There are two switches: one controlled (realized by a transistor or MOSFET) and one uncontrolled (realized by a diode). When the transistor is turned "on," the diode is turned off, and current flows through the inductor and the load. When the transistor is turned off, current flows freely through the diode and decays. Continuous current operation is achieved by correctly selecting the on-off frequency and inductor value, and the output voltage is then given by[21].

$$V_o = V_s/(T_{on}/(T_{on} + T_{off})) \quad (2.20)$$

The figure 2.8 below shows the structure of buck converter.

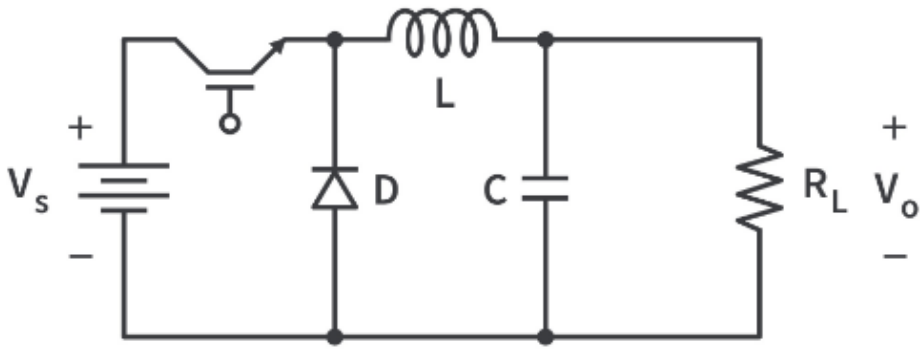

Figure 2.8: buck converter.

Whenever the switch is on, Vo= Vs+V_L and whenever the switch is off, Vo= V_L. The switch is on for a specific amount of time DT (where D - 1) and off for the remainder of the time (1-D)T for each time interval T. D here refers to the switch's duty cycle frequency[22].

2.2.2.1 Operation of the Buck Converter

The figure 2.9 and figure 2.10 shows the working of a buck converter.

When the switch is closed (0 to DT)

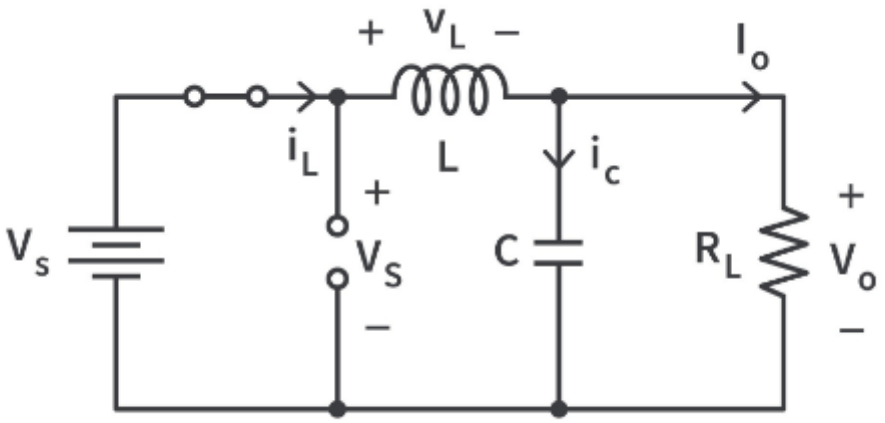

Figure 2.9: closed switch buck converter.

Using KVL to determine V_L, we get

$$V_L = V_S - V_0 = L\frac{di_L}{dt} \quad (2.21)$$

$$\frac{di_L}{dt} = \frac{V_S - V_0}{L} \quad (2.22)$$

di_L/dt is a positive constant since $V_S > V_o$) hence the inductor current increases linearly. Some part of i_L charges the capacitor to V_o while the rest flows through the load as the load current I_o.

After integration we will get the following equation:

$$i_L = \frac{V_S - V_0}{L}\ t + i_{Lmin} \quad (2.23)$$

At time t =0 the inductor current has a minimum value $i_L(0) = i_{Lmin}$, and increases

until reaching the i_{max} value at time t →DT.

$$i_{Lmax} = \frac{V_S - V_0}{L} DT + i_{Lmin} \quad (2.24)$$

Ripple current :

$$\Delta i_L = i_{Lmax} - i_{Lmin} \quad (2.25)$$

$$T = \frac{1}{f} \quad (2.26)$$

$$\Delta i_L = \frac{V_S - V_0}{Lf} D \quad (2.27)$$

Equation shows that to decrease the ripple current it is necessary to increase the switching frequency.

- **When the switch is open (for DT < t < T)**

The inductor tries to keep current flowing in the same direction as before, forward biasing the diode in the process. The inductor current now has a freewheeling path through to the diode.

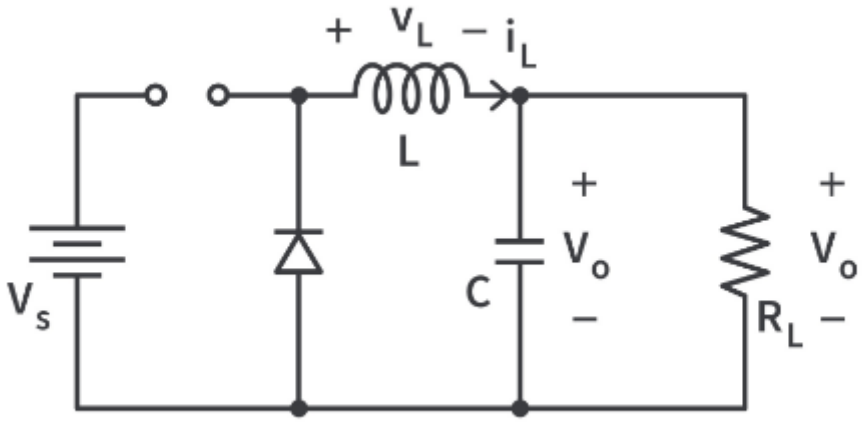

Figure 2.10: open switch buck converter.

Using KVL to determine V_L, we get

$$V_L = -V_0 = L\frac{di_L}{dt} \quad (2.28)$$

It is important to note that diL/dt is a negative constant. The inductor discharges the energy stored in it from when the switch was closed and the current decreases linearly in this duration with time. During this time, the capacitor keeps the output at Vo because it was charged to Vo when the switch was closed. When the switch is off, the inductor ensures that the load current continues to flow, and the high value of capacitance ensures that the output is maintained at Vo throughout.

After integration of KVL, we will get

$$i_L(t) = \frac{-V_0}{L}t + i_{Lmax} \quad (2.29)$$

When t = T the current of the inductor decreases from its maximum value to a minimum value.

$$i_{Lmin} = \frac{-V_0}{L}(1-D) + i_{Lmax} \quad (2.30)$$

The determination of the ripple current:

$$\Delta i_L = \frac{V_0}{Lf}(1-D) \quad (2.31)$$

$$\frac{V_0}{Lf}(1-D) = \frac{V_S - V_0}{Lf} D \quad (2.32)$$

$$V_o = DV_s \quad (2.33)$$

This equation shows us that the variation of the output voltage is a function of the duty cycle when D is varied from 0 to 1 the output voltage varies linearly from 0 to the input voltage value[22, 23].

2.2.3 Buck-Boost converter

A high efficiency and low ripple DC-DC converter is needed in the system for residential power production to achieve a stable voltage from an input source (PV cells) that is higher and lower than the output. Buck-Boost converters make it possible to convert a DC voltage to either a lower or higher voltage, and they do so quite effectively. Buck boost converters are particularly helpful for tracking the maximum power of a PV system.
In these instances, the goal is to get the maximum amount of power out of the solar panels at all times, regardless of the type of load.

A buck boost converter, which can be step up (Boost) and step down (Buck), can be acquired by cascading the connection of two basic converters. Buck type converters are commonly used in PV systems for charging batteries. The boost converter, on the other hand, is used to increase the voltage. Before the inverter stage, grid-connected devices use a boost type converter to step up the output voltage to the utility level. The benefits of buck-boost converter are:

- Buck-boost DC-DC switching converters are ideal for high-efficiency household appliances.
- Minimum ripple voltage.[24]

The figure 2.11 below shows the buck boost converter

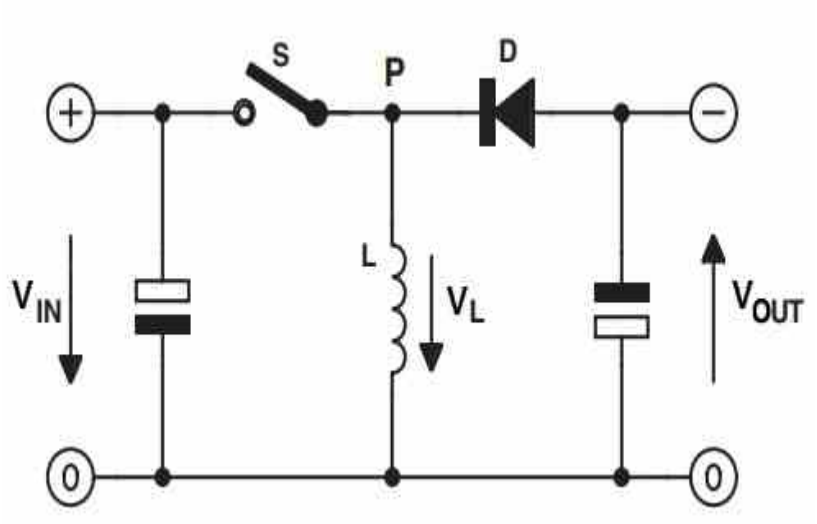

Figure 2.11: buck boost converter.

The switch conducts the inductor current and the diode becomes reverse biased when it is on for the duration DT, where $DT$is the duration and $D$is the duty ratio. Across the inductor, a voltage $V_L = V_{in}$ is produced. The inductor current I_L increases as a result of this voltage. Due to the inductor's energy storage, the inductor current I_L keeps flowing even after the switch is switched off. The voltage across the inductor changes to $V_L = -V_o$ for the duration of $(1 - D)T$ until the switch is turned back on as a result of this current flowing through the diode[25].

Table 2.1: Dc Dc converters and their duty ratio.

DC DC converter	Duty ratio
Buck	D
Boost	$\frac{1}{1-D}$
Buck boost	$\frac{-D}{1-D}$

2.3 MPPT tracking

Different types of techniques have been used for tracking the MPPT of PV system such as perturb and observe(P&O) and incremental conductance, etc. Under certain atmospheric

conditions, the incremental conductance method is complex but more effective than P&O method in PV systems[26].

The figure 2.12 shows the working Principe of MPPT.

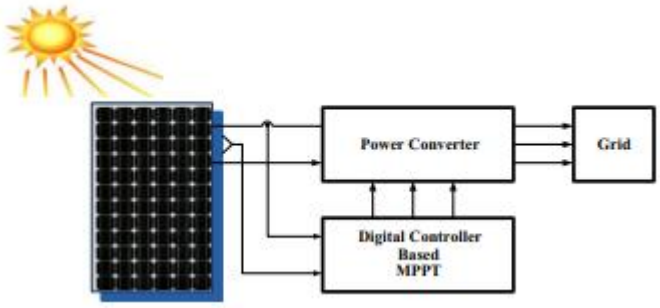

Figure 2.12: MPPT working Principe.

2.3.1 MPPT Solar Charge Controller

The MPPT controller is the device that manages the PV in order to get the maximum power possible. The effectiveness of the PV system is increased if the controller operates deliberately at MPP, regardless of the environmental conditions. To achieve maximum power output, it should be possible to legitimately match the PV source with the load for any climatic condition. The PV array can be powered to its maximum efficiency using either mechanical tracking or electrical tracking. In mechanical tracking, the PV panel direction changes according to the changes of months and seasons throughout the year, while in electrical tracking, the I V curve is used for locating MPP[27–29]. Modern power systems must include MPPT in order to guarantee that the maximum amount of power reaches the load, batteries, motors, and the power grid for off-grid and on-grid applications, respectively[29].

2.3.2 Battery

Electrochemical devices that convert chemical energy into electrical energy are known as batteries. We can tell the difference between primary and secondary batteries. Primary batteries irreversibly convert chemical energy to electrical energy. Primary batteries include zinc carbon and alkaline batteries.

Secondary batteries, often known as rechargeable batteries, convert chemical energy to electrical energy in a reversible manner. This means that when an over potential is used, they can be recharged. In other words, excess electrical energy is stored as chemical energy in these

secondary batteries. Lead acid or lithium ion batteries are common examples of rechargeable batteries. Only secondary batteries are of interest in PV systems[30].

The battery's main purpose is to store the modified charge from the solar charge controller for later use. The most important aspect of solar energy is choosing the correct type of battery. As a result, the deep cycle type battery is preferred in this situation due to its efficiency. Deep cycle batteries are essentially energy storage units in which chemical reactions occur that produce voltage and thus electricity. It is named deep cycled because it operates in two cycles which are charging cycle and discharging cycle.

2.3.3 Several ways to track for MPP.

2.3.3.1 Direct methods

2.2.3.1.1 Perturb & Observe (P&O) MPPT algorithm

P&O is an iterative MPPT tracking technique. It senses the panel operating voltage periodically calculates and compares the PV output power with that of the previous power, then the operating voltage is changed by changing the duty ratio and change in the direction of power is noted to track MPP. The sign of the change in power is used; if the power increases by increasing the voltage, the operating voltage is further perturbed in the same way as shown in Fig below, and this process is repeated until dP/dV=0 is reached. As soon as the MPP is achieved, the voltage oscillates around it rather than being stably positioned on it, because voltage perturbation continues at the MPP as well. This is one of the most significant disadvantage of this technique. Furthermore, as the voltage is occasionally perturbed, significant power loss occurs[31]. In any case if there is any shadow on any of the panels (as they are in series of parallel)then the power-voltage curve of the PV will have several peaks and the P&O will not be able to distinguish them and find the genuine peak[24].This method, however, has the advantage of its simplicity and not needing solar panel characteristics. PV panel output voltage $V_{pv}$and output current $I_{pv}$are detected. Then power is calculated P(n) and compared with the power measured in the previous sample P(n-1), in order to get ΔP. The duty cycle of the converter is then changed to track MPP based on the sign of ΔP and ΔV, as summarized below:

- If the value of ΔP is zero, the system is working at MPP and no change in duty cycle is required.
- If the value of ΔP>0 and ΔV>0, the operating point is located on the left of MPP and duty cycle is to be decreased to increase the voltage so as to reach MPP.

- If the value of ΔP>0 and ΔV<0, the operating point is toward right of MPP and duty cycle must be increased to reach MPP.
- If the value of ΔP<0 and ΔV<0, the operating point is towards left of MPP and duty cycle is to be decreased to reach MPP.
- And if the value of ΔP<0 and ΔV>0, the operating point is towards right of MPP and duty cycle this time is to be increased to reach MPP.

The figure 2.13 below shows the flowchart of perturb and observe algorithm.

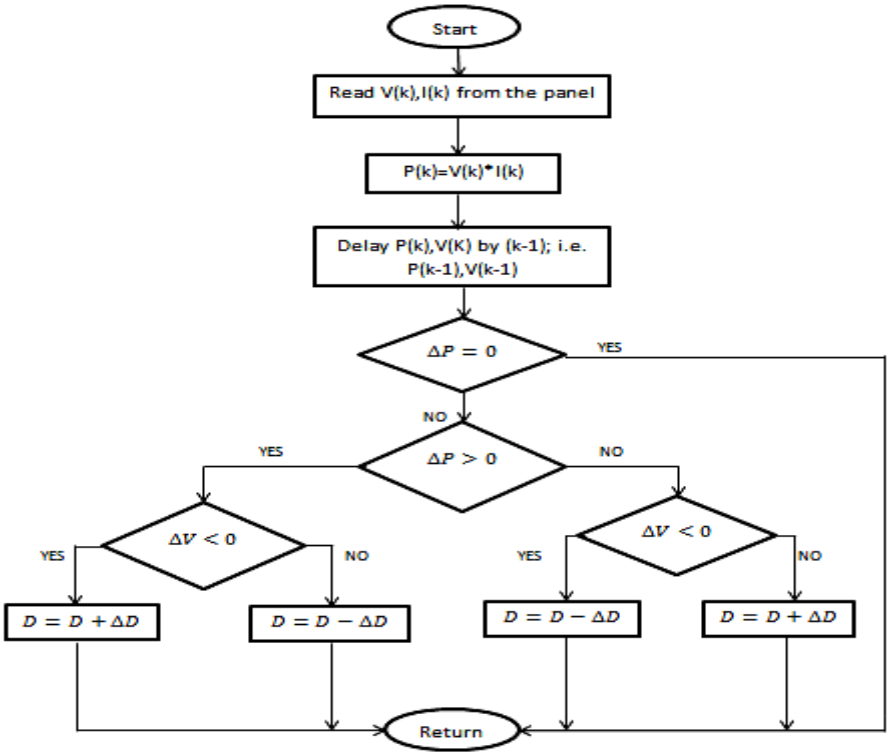

Figure 2.13: flowchart of perturb and observe algorithm.

The figures 2.14 and 2.15 explains the working of the Pertub and Observe algorithm.

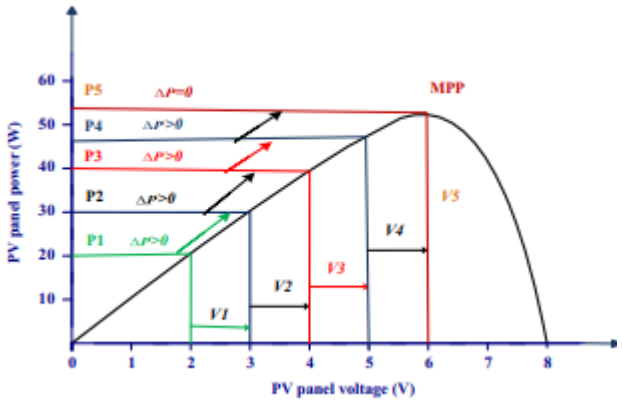

Figure 2.14: P–V Curve for P&O algorithm.

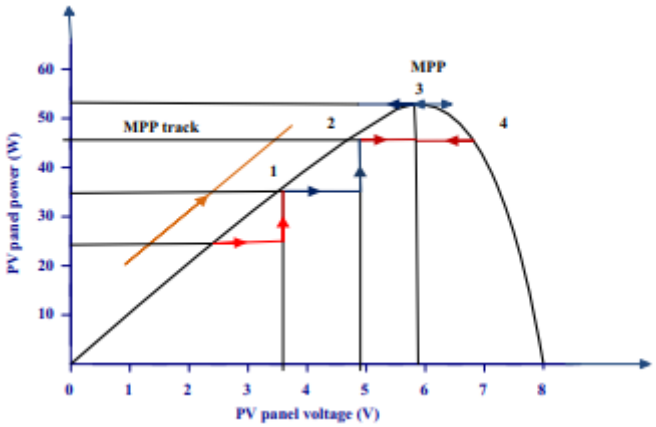

Figure 2.15: Implementation of P&O method, showing oscillations around MPP.

The conventional P&O method tracks the MPP by perturbing the PV panel voltage or current and moving the control variable towards the MPP with a fixed step size. Fixed step size tracking has some drawbacks, such as slow speed and large steady state oscillations[28]. If large steps are chosen, it will result in faster dynamics but steady state oscillations also increases and efficiency decreases[32]. However, if small steps are chosen, dynamics will slow down. To overcome the fixed step issue, adaptive (modified) P&O algorithms are used, which use adaptive step size to increase tracking speed and decrease steady state oscillations[28].

2.2.3.1.2 Incremental conductance method (INC)

INC technique is widely used MPPT technique. The disadvantage of the P&O technique of oscillation of the operating point around the MPP during changing environmental conditions can be eliminated by comparing the instantaneous conductance I_{pv} / V_{pv} with the incremental conductance (dI_{pv}/dV_{pv}). The voltage of MPP is tracked to satisfy dP_{pv} /dV_{pv} = 0, which is MPP. The INC-based algorithm is superior to other conventional methods because it is simple to apply, has a high tracking speed, and is more efficient[33].

Output power from solar array is:

$$P_{pv}=V_{pv}I_{pv} \tag{2.34}$$

Differentiating with respect to V_{pv} $gives$:

$$dP_{pv}/dV_{pv} = I_{pv} + V_{pv}\left(\frac{dI_{pv}}{dV_{pv}}\right) \tag{2.35}$$

At MPP:

$$\frac{dP_{pv}}{dV_{pv}} = 0 \tag{2.36}$$

$$\frac{dI_{pv}}{dV_{pv}} = -I_{pv}/V_{pv} \tag{2.37}$$

If the operating point is on the right of the power curve, then we have

$$dP_{pv}/dV_{pv}<0 \tag{2.38}$$

If the operating point is on the left of the power curve, then we have

$$\frac{dP_{pv}}{dV_{pv}} > 0 \tag{2.39}$$

The figure 2.16 below shows the working of INC conductance.

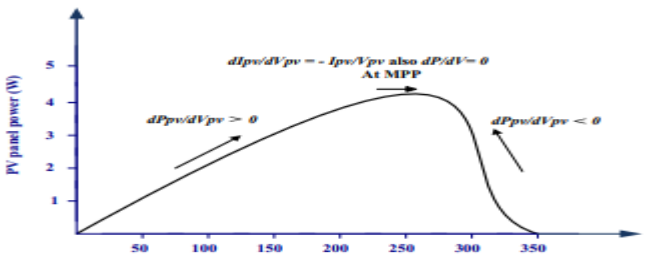

Figure 2.16: P–V curve for INC MPPT.

In this algorithm the present and previous values of the solar panel voltage and current are sensed and are used to calculate the values of $dI_{pv}\ and dV_{pv}$. If $dV_{pv} = 0\ and\ dI_{pv} = 0$, then there is no change in atmospheric conditions and the MPPT is still operating at MPP where $\frac{dP_{pv}}{dV_{pv}} > 0$,reference voltage is equal to maximum voltage for this atmospheric condition and is not changed that is there is no perturbation until a change in current is sensed. In order to track the MPP, the duty cycle of the DC/DC converter is adjusted, changing the PV operating voltage. The problem of fixed small or large steps can be resolved, if MPPT with variable step size is used, as recommended by the variable step size (Modified) INC MPPT algorithm, adjusts the step size automatically in accordance with the characteristics of the PV array[28, 33]. When the operating point is far from the MPP, the step size is raised, allowing for quick tracking; however, when the operating point is close to the MPP, the step size decreases, reducing oscillations and increasing efficiency. With few oscillations and a good balance between dynamic and steady state response, this method produces excellent results in rapidly changing atmospheric conditions[33].

The figure 2.17 below shows the flow chart of INC algorithm.

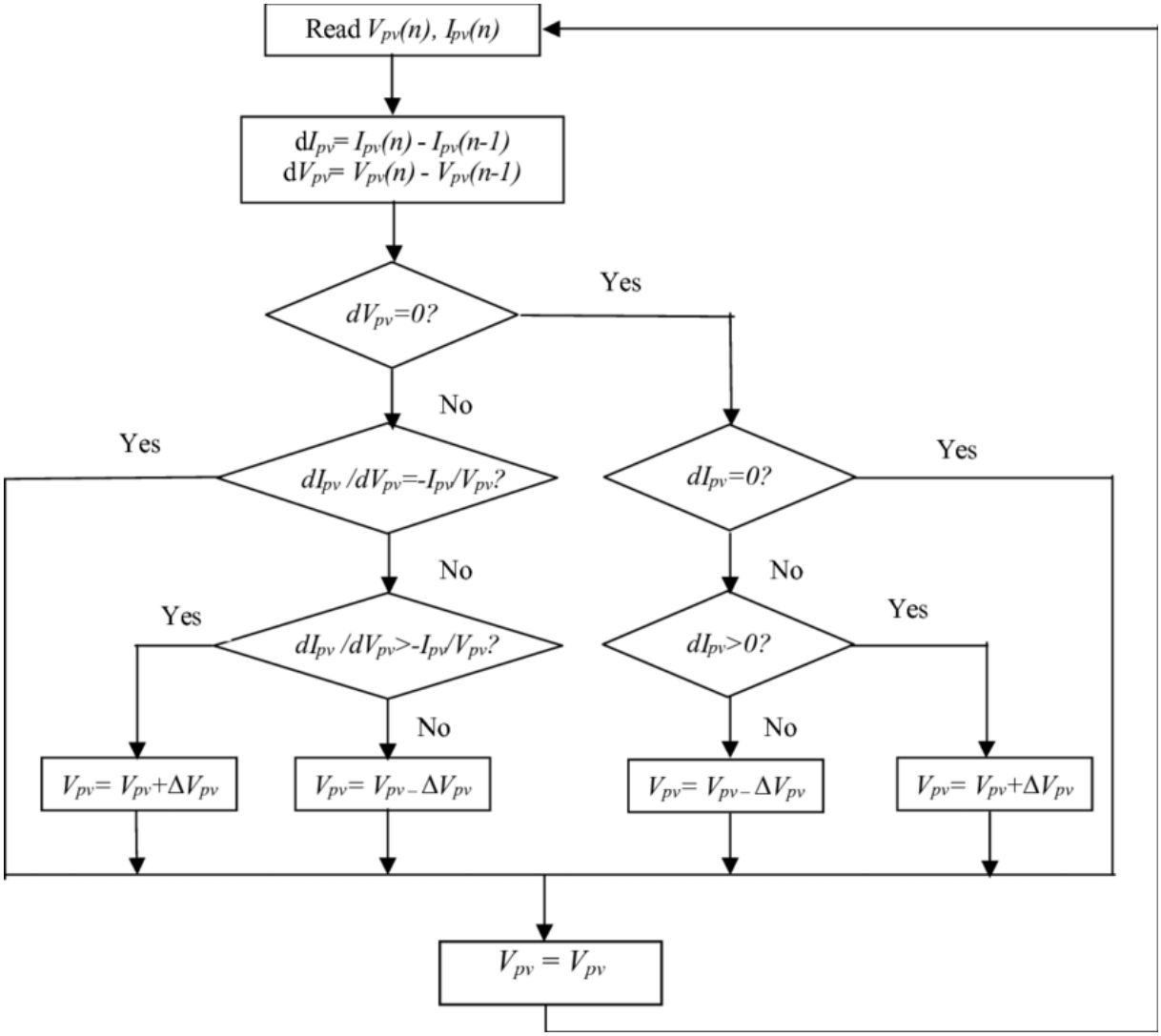

Figure 2.17: INC Algorithm.

2.3.3.2 Indirect methods

2.3.3.2.1 Constant Voltage method

Although very simple, the constant voltage technique is ineffective. In this approach, the V_{mpp} is just represented by a single voltage. In some instances, an external resistor connected to the control IC's current source pin sets this value. About 80% of the maximum power is collected by the technique for each of the different irradiance variations. The average irradiance level will decide the actual performance. The tracking efficiency is poor in this instance because the maximum power point of a solar module does not always fall between 70 and 80 percent of Voc.

The figure 2.18 below shows the flowchart of constant voltage method.

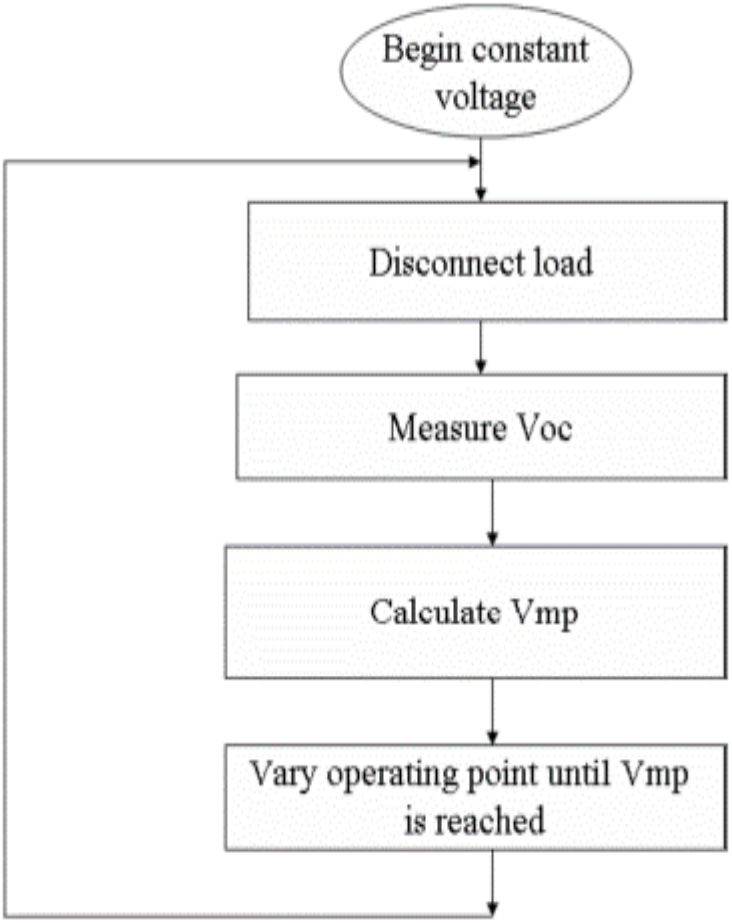

Figure 2.18: Flowchart of constant voltage method.

2.3.3.2.2 Open Circuit Voltage Method

The Open Circuit Voltage method, which uses a similar concept to the Constant Voltage method but with some improvements. It uses V_{oc} to calculate V_{mpp}. Once the system obtains the V_{oc}value, $V_{mpp}$is calculated by,$V_{mpp} = K * V_{oc}$ as shown in figure 2.19 below.

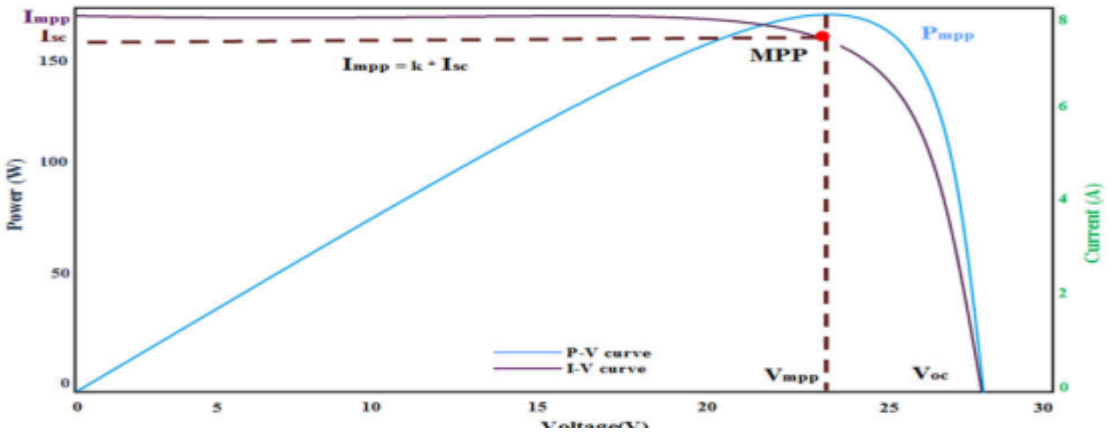

Figure 2.19: I-V and P-V characteristics of Open circuit voltage method.

The V_{oc} represents the PV panel's open circuit voltage. Because the k value is always less than unity, it usually ranges from 0.7 to 0.8 (commonly used as 0.76). It is necessary to update V_{oc}occasionally to compensate for any temperature change and irradiance. When the input current is monitored, it can show when the V_{oc}should be re-measured. The k value is a logarithmic function of the irradiance that rises in value as the irradiance increases. The benefits of using this method is relatively low cost and easy to implement. There are also drawbacks to this method such as not operating exactly at maximum power point. It is not a very accurate method[24].

2.4 Conclusion

By implementing MPPT algorithms, PV systems can optimize power extraction, improve the efficiency and improve overall system performance. Both direct and indirect methods in MPPT have their advantages and limitations.

In the next chapter, simulation of PV system with MPPT algorithm will be presented.

Chapter 3: Modelisation and simulation of photovoltaic solar panel

3.1 Introduction

The PV panel model based on electrical equivalent circuit aspect is described and give a thorough analysis of one diode model and its practical verification. The two diode model is more accurate and gives a model with I-V characteristics that are closer to the practical behaviour of a PV cell. However, the two diode model is more complex and requires more computational effort than the one diode model. As a result, one diode model-based analysis is common in the literature. In this chapter, we have used one diode model to simulate the PV system in proteus.

3.2 Equivalent circuit based modeling

The one-diode solar cell concept in which the quantity of electrical energy produced by the PV cell is represented by a current I_{ph}that is proportional to the amount of solar irradiation. Internal resistance is represented by series resistance, whereas leakage current is represented by shunt resistance[34].

In ideal single diode model:

The internal losses of the current are not taken into account by this model. A diode is connected in anti-parallel with the light generated current source. Kirchhoff law is used to determine the output current I:

The figure 3.1 below shows the ideal single diode model.

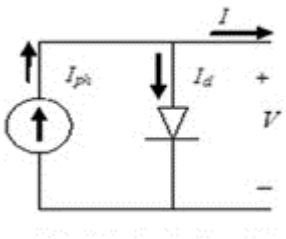

Figure 3.1: Ideal single diode model.

$$\mathrm{I} = \mathrm{I_{ph}} - \mathrm{I_d} \tag{3.1}$$

I_{ph} is the photocurrent, I_d is the diode current, which is determined by the equation below and is proportional to the saturation current:

$$\mathrm{I_d} = \mathrm{I_0}[\exp\left(\frac{\mathrm{V}}{\mathrm{A.N_S.V_T}}\right) - 1] \tag{3.2}$$

V imposes a voltage on the diode.

$$V_T = k.{}^{T_C}/_{q} \quad (3.3)$$

I_0 is the diode's reverse saturation or leakage current (A).

V_{TC}= 26 mV at 300 K for silisium cell,T_c is the actual cell temperature (K).

q is the electron charge (1.602×10^{-19}C), and k is the Boltzmann constant (1.381×10^{-23} J/K).

$V_T$is referred to as the thermal voltage because of its exclusive dependence of temperature.

N_S : the number of PV cells that are linked together in series. The ideality factor is A. It can be selected from Table below and depends on PV cell technology. The fact that A is a constant that depends on PV cell technology must be underlined[35].

A diode's ideality factor is a measure of how closely it follows to the ideal diode equation. Certain assumptions about the cell are made in the derivation of the simple diode equation[36].

Table 3.1: ideality factors for different solar cell technology[37].

Solar cell technology	Ideality factor
Silicon monocrystalline	1.20
Silicon polycrystalline	1.30
Amorphous silicon (a-Si):H	1.80
Amorphous silicon (a-Si):H tandem	3.30
Amorphous silicon (a-Si):H triple	5.0
Cadmium Telluride(CdTe)	1.50

$$a = \frac{N_s.A.kT_c}{q} = N_s.A.V_T \quad (3.4)$$

While A is the diode ideality "a" is referred to as "the modified ideality factor"

The figure 3.2 shows the practical model with resistor in series.

In practical model with R_s

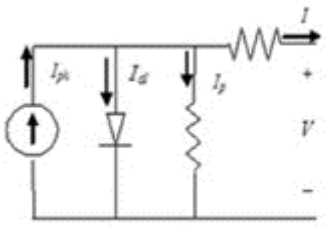

Figure 3.2: practical model with R_s.

Given their impact on the efficiency of the PV cell and the PV module, it is actually impossible to ignore the series resistance Rs and the parallel resistance RP. When RS is considered, equation should have the following form:

$$I_d = I_0[\exp(\frac{V+IR_s}{a})-1] \quad (3.5)$$

In practical model with $R_s and\ R_p$(real model) as shown in figure 3.3 below

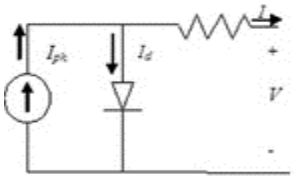

Figure 3.3: practical model with $R_s and\ R_p$.

By applying Kirchhoff law, current will be obtained by the equation:

$$I = I_{ph} - I_d - I_p \quad (3.6)$$

I_p, is the current leak in parallel resistor.

The output current of a module with Ns cells connected in series is:

$$I = I_{ph} - I_0\left[\exp\left(\frac{V+IR_s}{a}\right) - 1\right] - \frac{V+R_sI}{R_p} \quad (3.7)$$

This model has the best match with experimental results[35].

3.3 PV system simulation

The Proteus platform is one of the best and easiest software to implement for PV systems. Furthermore, Proteus software is one of the most commonly used simulation software due to its ease of use and wide range of various electronic components. The Arduino UNO board is one of the components that can be used flexibly in the Proteus software.

I had a simulation block developed using "Proteus" software (by ISIS) based on the equivalent circuit of a PV generator.

3.3.1 Implementation of a PV Generator on Proteus

Parameters of BLD Solar at standard test conditions

Table 3.2: Parameters of BLD Solar panel.

Type		BLD200 72M
Maximum Power	P_{max}	200W
Output Tolerance		±3%
Current at Pmax	I_{mp}	5.29A
Voltage at Pmax	V_{mp}	37.77V
Short Circuit Current	I_{sc}	5.92A
Open Circuit Voltage	V_{oc}	45.25V
Nominal Operating Cell Temp	T_{noct}	45±2 °C
Weight		15KG
Dimension		1580*800*35mm
Maximum system voltage		1000V
Maximum series fuse rating		10A
Cell Technology		MONO Si

3.3.1.1 Modeling one-diode PV model in proteus software at STC:

In order to replicate a reliable PV panel model in Proteus software, the equivalent circuit of a single diode should be taken into account along with a striped current source to represent the photocurrent source, a single diode with modified spice code, and series and parallel resistances.

The PV panel model in Proteus software with a one-diode model is shown in the figure below:

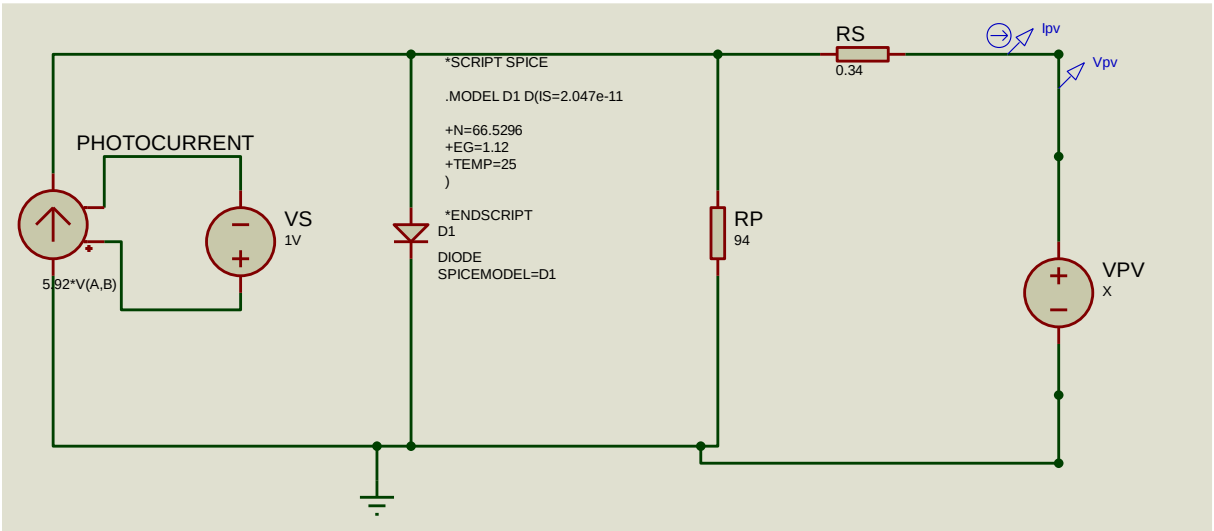

Figure 3.4: one diode PV model in proteus.

The graphs of the solar panel used in this simulation are as shown in figure 3.5 and figure 3.6.

The IV curve of the solar panel

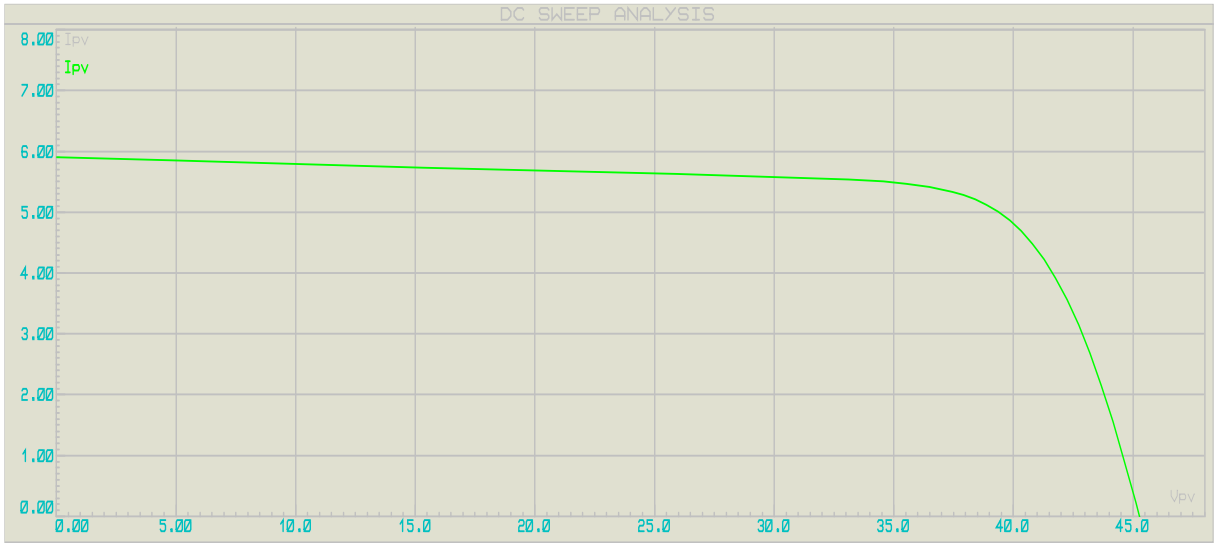

Figure 3.5: The IV curve of the solar panel.

The PV curve of a solar panel

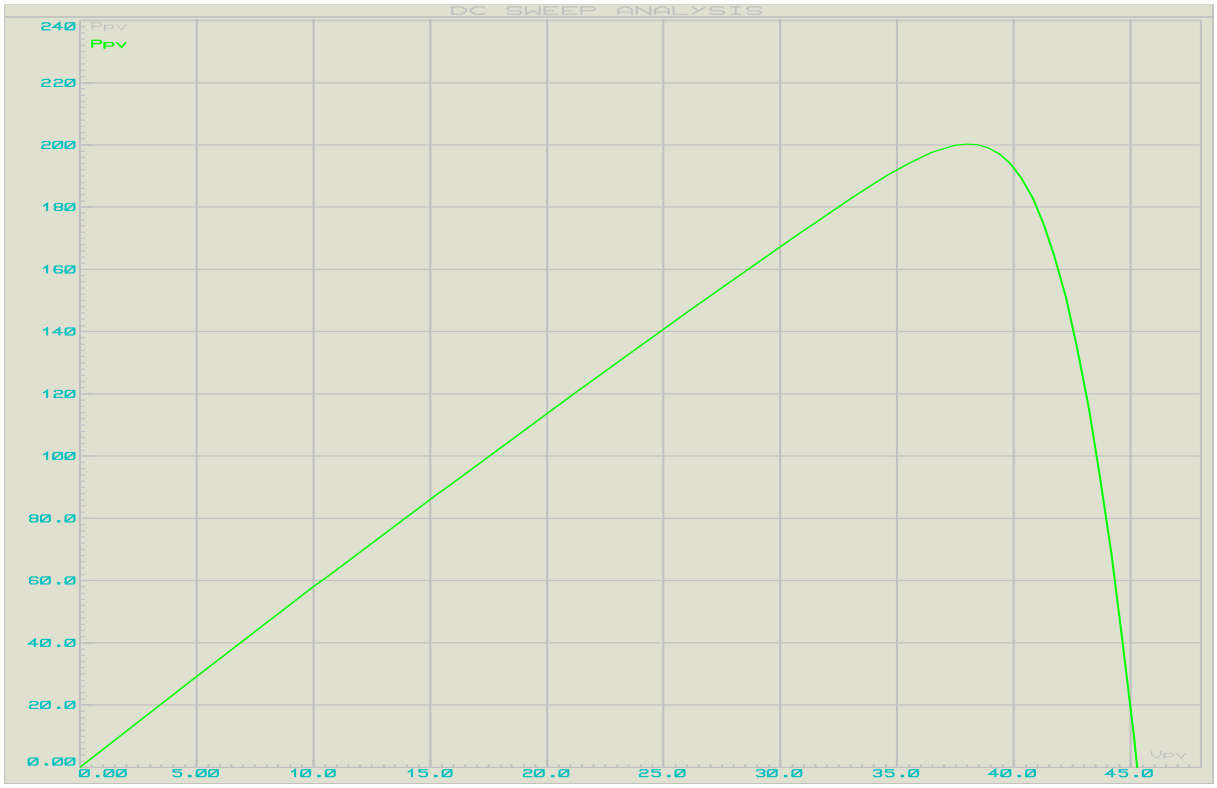

Figure 3.6: The PV curve of a solar panel.

3.3.1.2 DC-DC boost converter in Proteus

The figure 3.7 below shows the circuit diagram of boost converter in proteus.

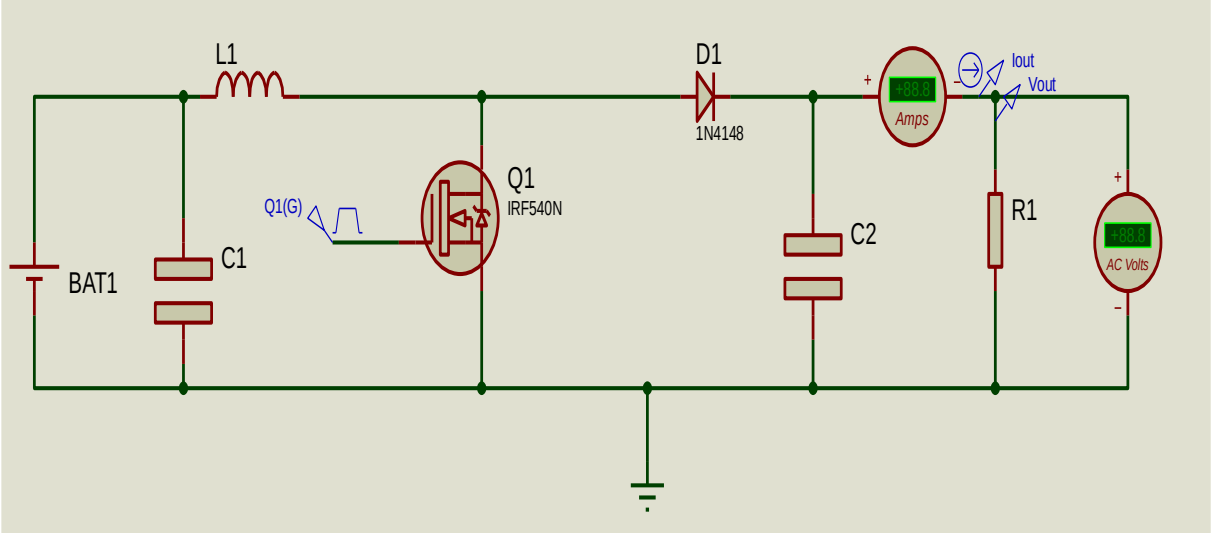

Figure 3.7: DC-DC boost converter in Proteus.

The valeurs I have used in this simulation are:

$$C_i \geq \frac{4\,V_{mp}D_{mp}}{\triangle V_i R_i f_s} = 775\mu F \text{ only for } 1000W/m^2 \quad (3.8)$$

$$C_o \geq \frac{2\,D_{mp}}{\triangle V_o R_o f_s} = 115\mu F \text{ only for } 1000W/m^2 \quad (3.9)$$

$$L \geq \frac{V_{mp}D_{mp}}{2\triangle I_o f_s} = 3.35mH \text{ only for } 50W/m^2 \quad (3.10)$$

$C_{in} = 1500\mu F$

$C_{out} = 150\mu F$

$L = 40mH$[38].

3.3.1.3 PV system simulation block diagram at STC ((1000/m^2 and 25°C):

The Arduino inputs are connected with a current sensor and a voltage divider (voltage sensor). The overall PV system simulation is shown in Figure below.

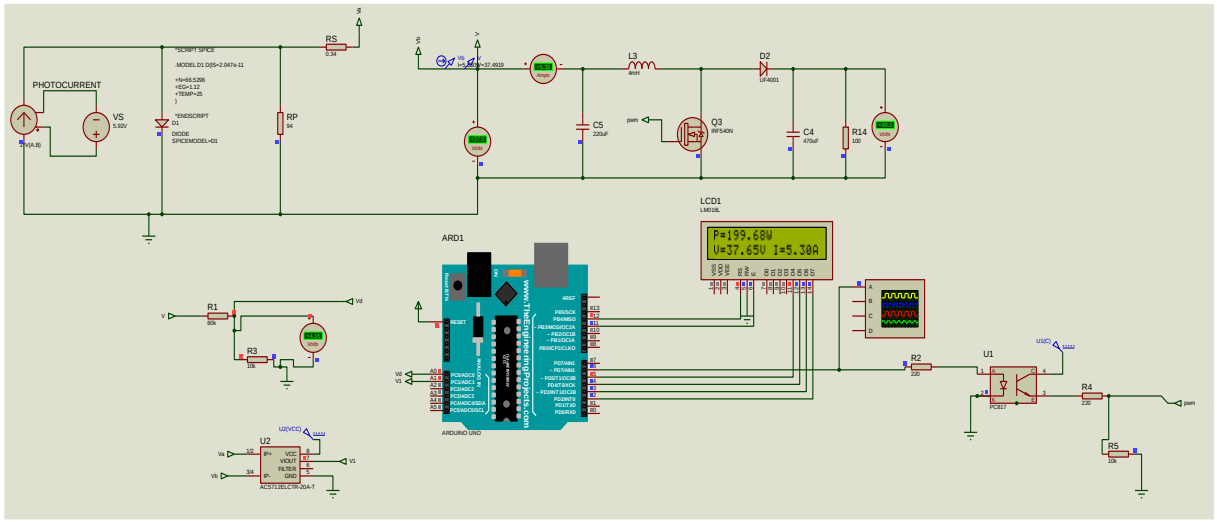

Figure 3.8: MPPT PV system simulation in proteus.

3.3.1.4 Results of simulation:

The figure 3.9 below shows the graph of Voltage(V) in function of time(s) for 100 Ohm load.

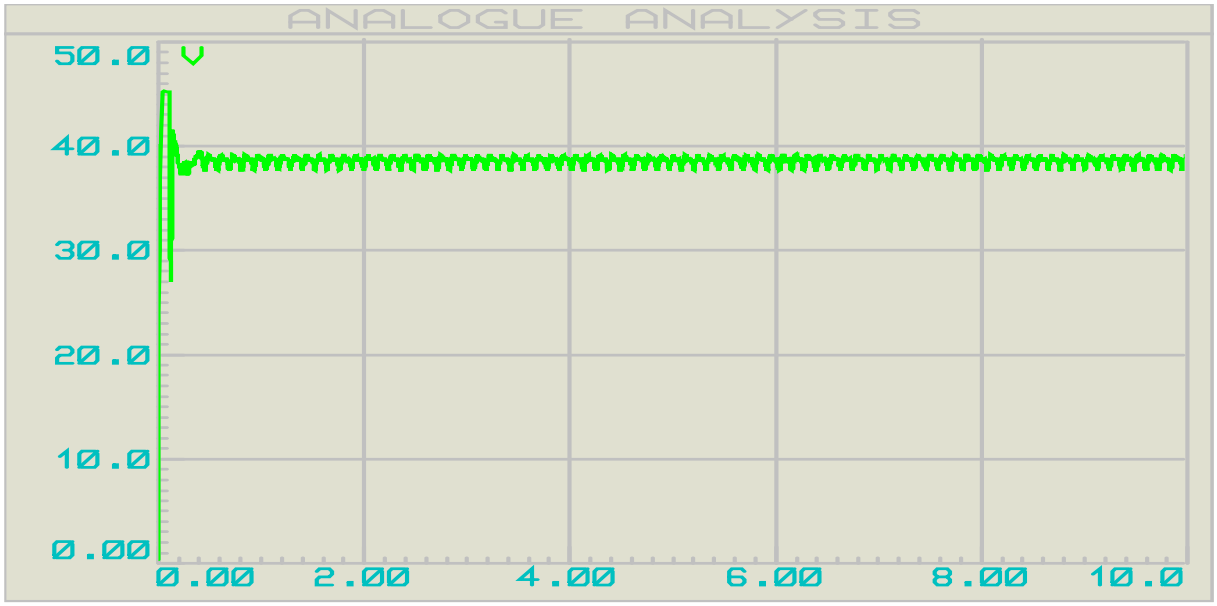

Figure 3.9: PV voltage under STC for P&O technique with 100Ω load.

The figure 3.10 below shows the graph of Voltage(V) in function of time(s) for 50 Ohm load.

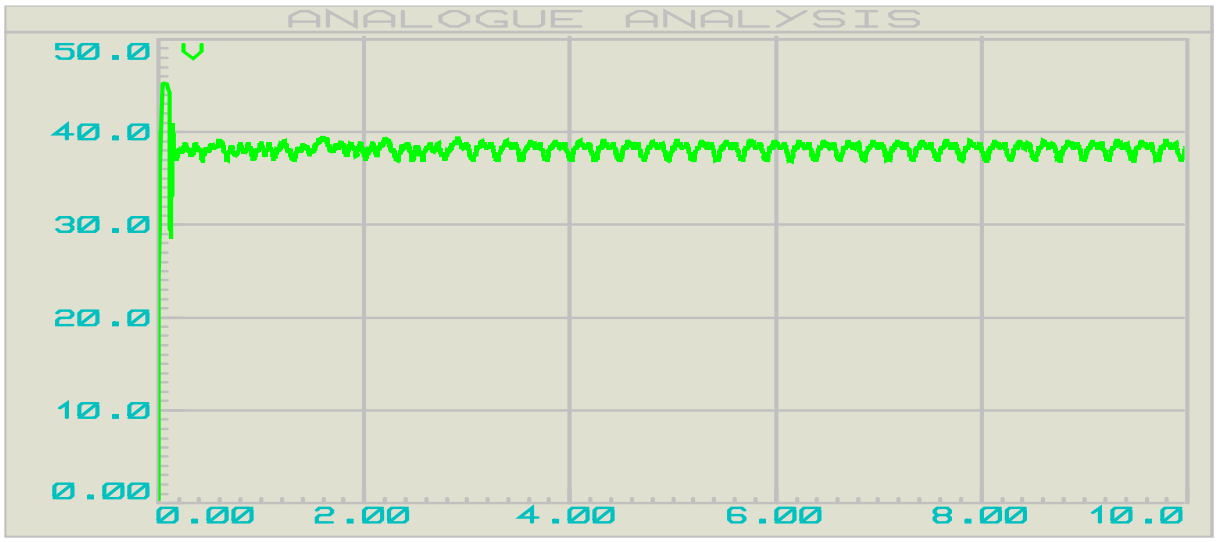

Figure 3.10: PV voltage under STC for P&O technique with 50Ω load.

We note that the value of voltage increases until it reaches the optimum voltage ,it starts oscillating around optimum voltage.

The figure 3.11 and figure 3.12 below shows the graphs of Power(W) in function of time(s) for 100 Ohm and 50 Ohm loads respectively.

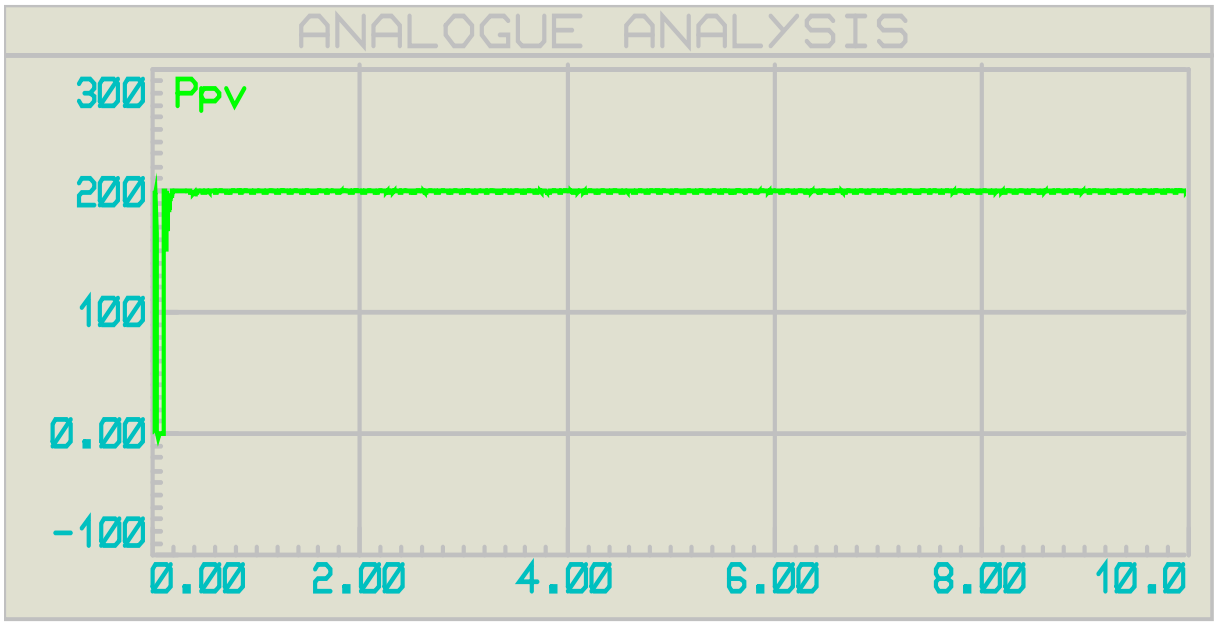

Figure 3.11: PV power under STC for P&O technique with 100Ω load.

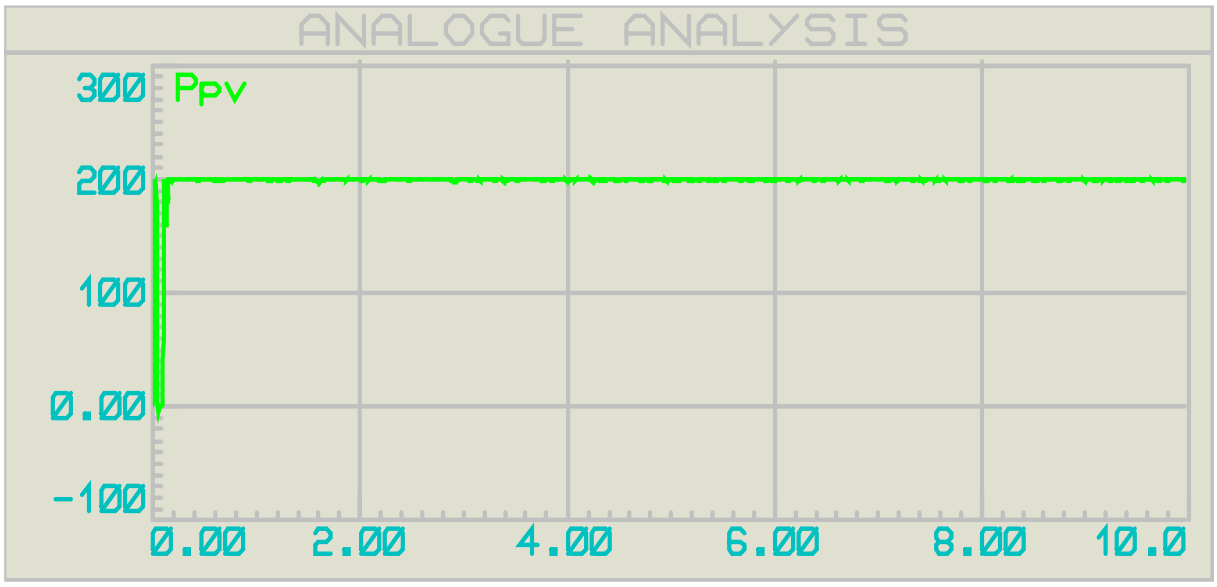

Figure 3.12: PV power under STC for P&O technique with 50Ω load.

We note that the value of power increases until it reaches the maximum power ,it starts oscillating around maximum power.

3.3.1.5 PV system simulation diagram at variable irradiance(1000/m^2, 750W/m^2,560W/m^2) and constant temperature of 25°C:

The figure 3.13 and figure 3.14 below shows the complete circuit of simulation diagram at variable irradiance.

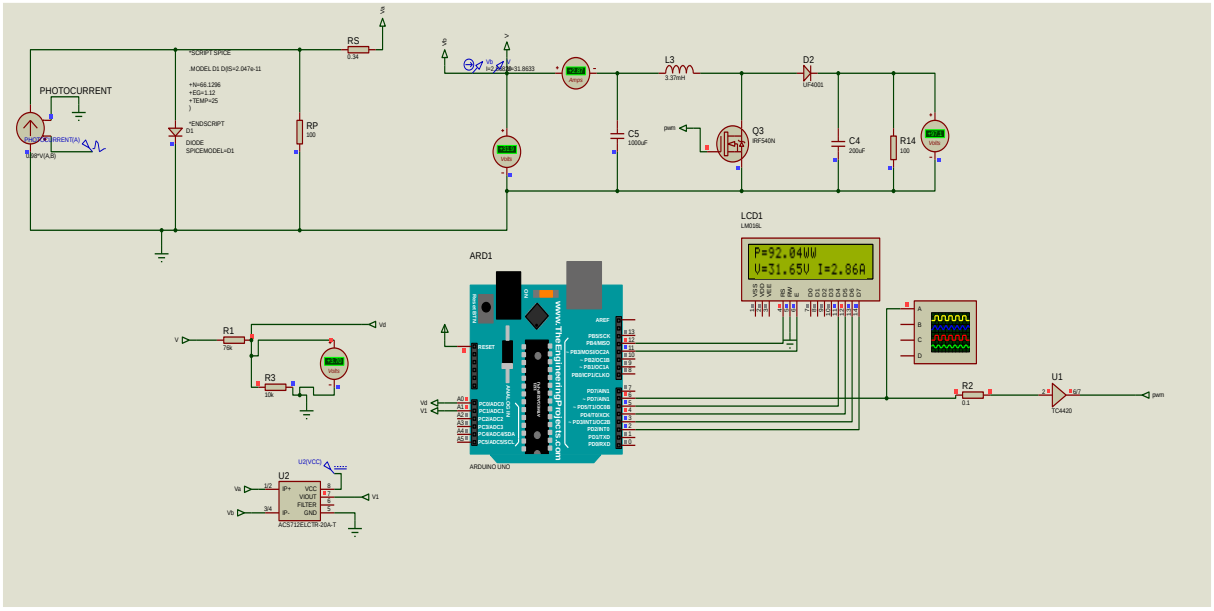

Figure 3.13: PV system simulation block diagram at variable irradiance.

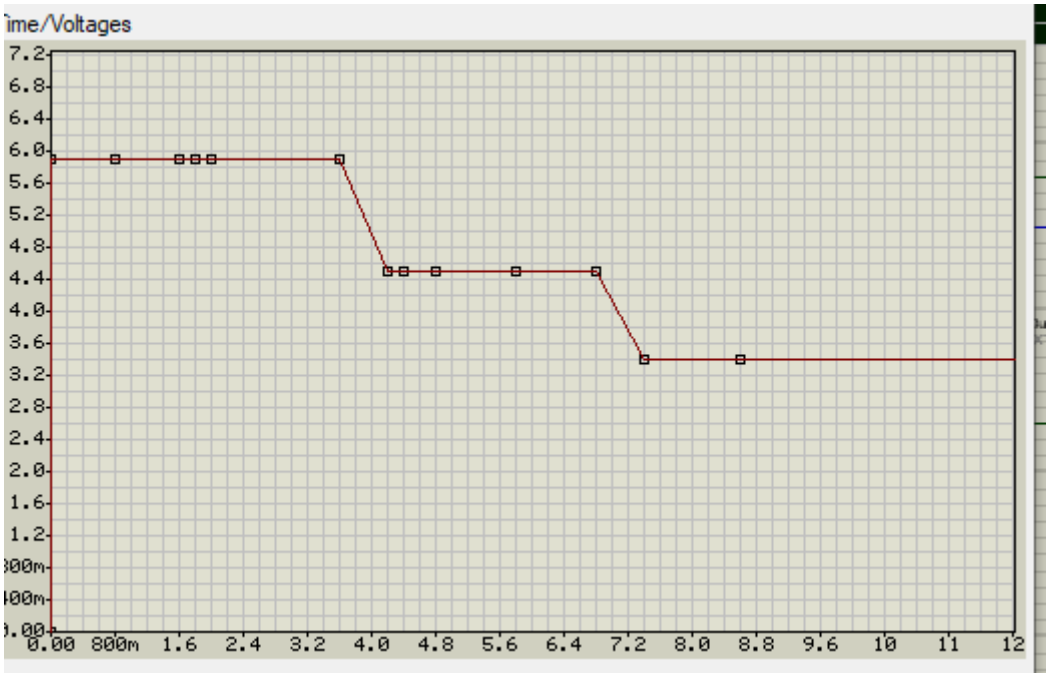

Figure 3.14: Variation of irradiance.

3.3.1.6 Results of simulation:

The figures 3.15 and 3.16 shows the graph of voltage(V) in function of time(s) for 100 Ohms and 50 Ohms respectively .

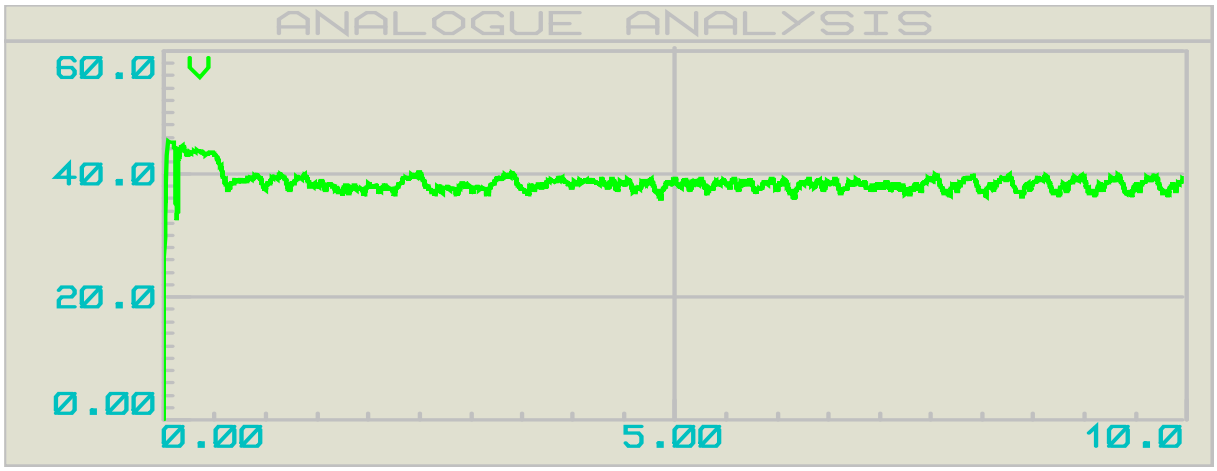

Figure 3.15: analogue analysis of PV voltage under variable conditions for P&O technique with 100Ω.

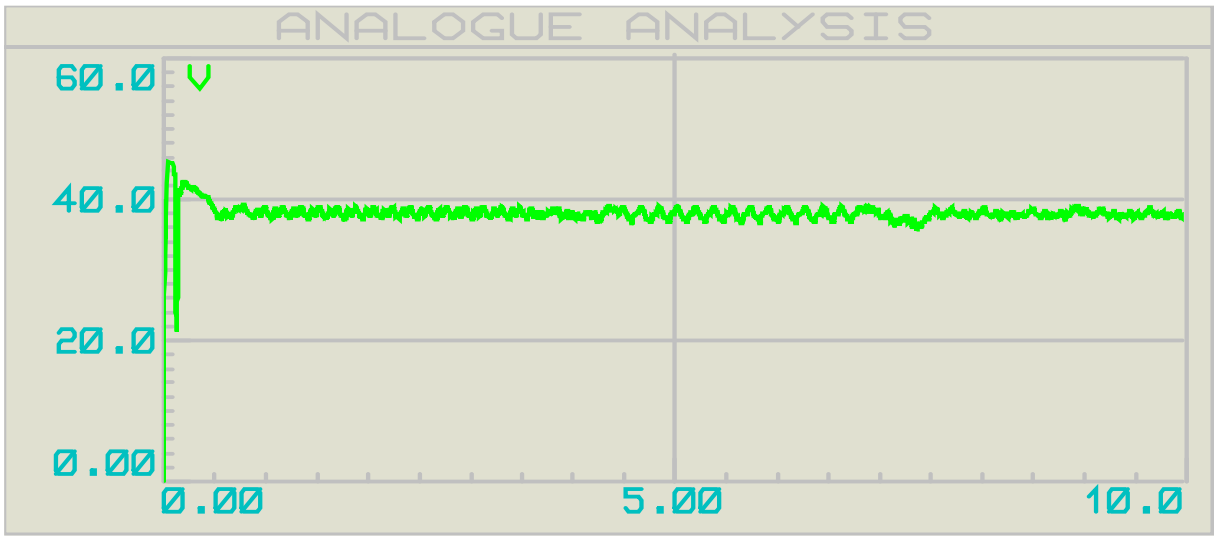

Figure 3.16: PV voltage under variable conditions for P&O technique with 50Ω load.

We note that the value of voltage increases until it reaches the optimum voltage ,it starts oscillating around optimum voltage.

The figures 3.17 and 3.18 below shows the graphs of Power(W) in function of time(s) for different irradiances for 100 Ohm and 50 Ohm respectively.

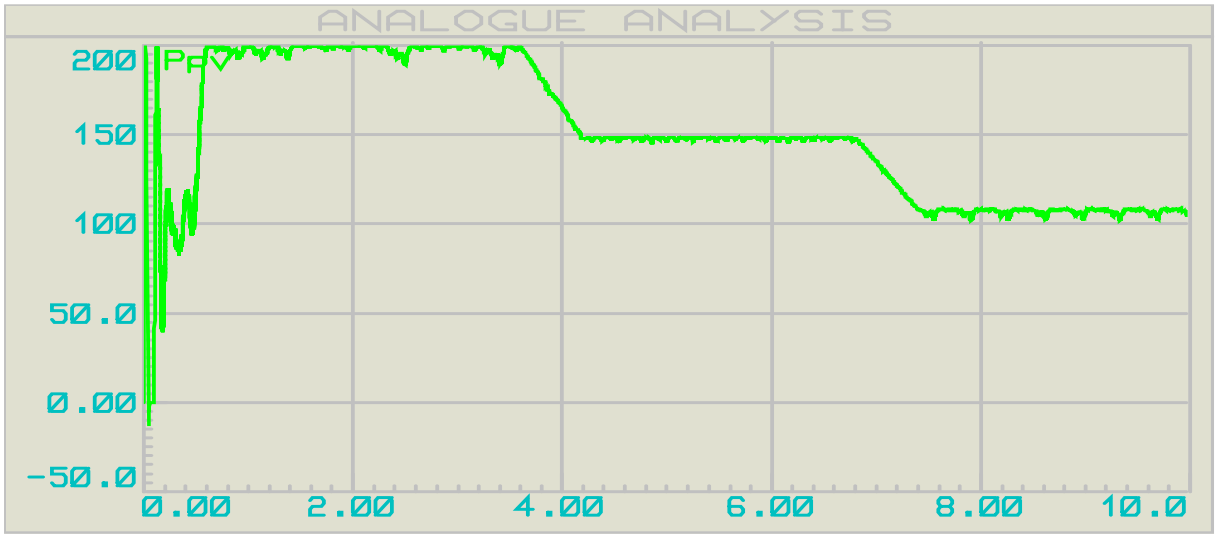

Figure 3.17: PV Power under variable conditions for P&O technique with 100Ω load.

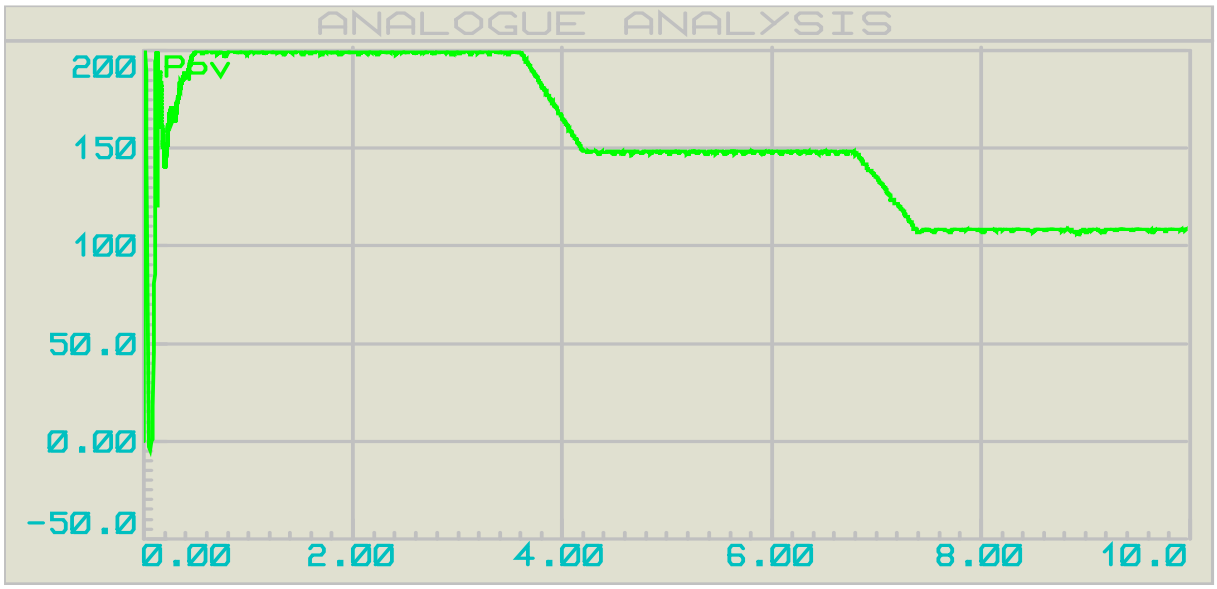

Figure 3.18: PV Power under variable conditions for P&O technique with 50Ω load.

3.3.1.7 Interpretation of results:

The Arduino varies the value of duty cycle by varying pwm according to the values of voltage and current picked up. We note that the value of the voltage is increased until reaches the maximum value. Then it stabilizes at this value. Also the power is increased as the voltage increases, then it stabilizes at maximum value of power. This stability proves that the principle of the MPPT command is verified. In the case of standard state conditions, the duty cycle varies until it reaches 0.5. The duty cycle oscillates between 0.48 and 0.5 due to oscillations of voltage at MPP with the load of 100Ω.When we replace the load with 50, the duty cycle oscillates between 0.42 and 0.45.

3.2 Conclusion:

The P&O algorithm exhibits good tracking efficiency under steady-state conditions. It can accurately track the maximum power point by perturbing the operating point and observing the change in power output. The P&O may exhibit oscillatory behavior around the MPP, particularly when they are sudden changes in environmental factors such as irradiance or temperature. These oscillations can result in fluctuations around the MPP.

In the next chapter, implementation of MPPT using P&O algorithm will be presented.

Chapter 4: Implementation of MPPT techniques

4.1 Introduction

In this chapter, we present the realization of the MPPT PV system with 3.8Watts solar panel and different electronic components of the system such as current sensor, voltage divider circuit, Arduino Uno, diode and mosfet.

4.2 Arduino UNO

The ATmega328P microprocessor is the foundation of the Arduino UNO. Compared to other boards, like the Arduino Mega board, etc., it is simple to use. The board is made up of shields, various circuits, and digital and analog Input/output (I/O) pins. The Arduino UNO has 14 digital pins, a USB port, a power jack, and an ICSP (In-Circuit Serial Programming) header in addition to 6 analog pin inputs. The programming language used is called IDE, or integrated development environment.

The components of Arduino UNO board are shown in the figure 4.1 below:

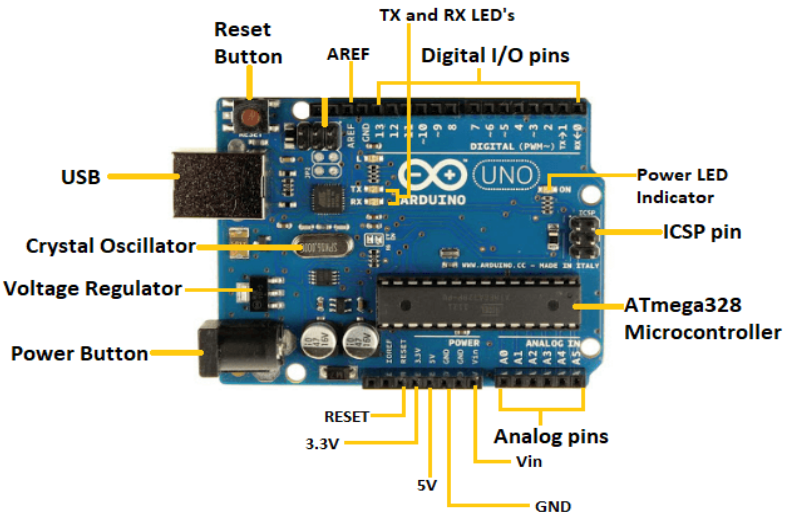

Figure4.1: Arduino Uno.

The Arduino board's USB connection is used to link the board to a computer through a USB cable. The cable functions as the board's power supply and serial port. Such dual functioning makes it unique to recommend and easy to use for beginners[39].

4.3 ACS 712 (0.5B) current sensor

The figure 4.2 below shows the current sensor used in the implementation of thi work.

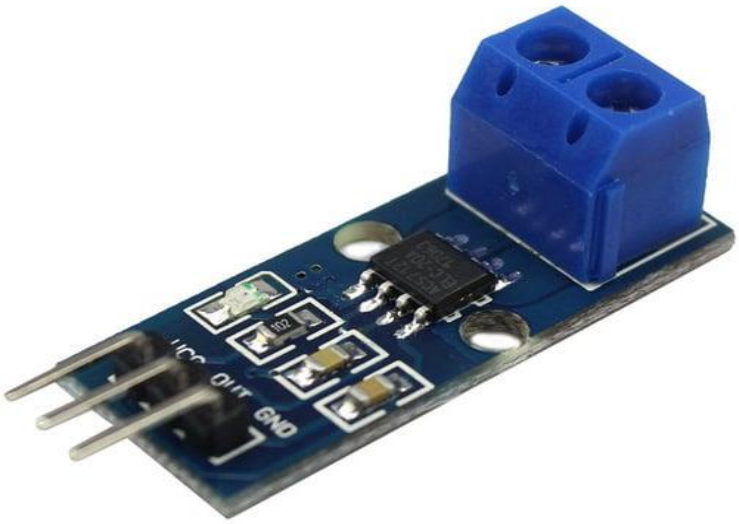

Figure4.2 : ACS 712 (0.5B) current sensor.

This module is based on the ACS712ELC-0.5BA integrated circuit, a high performance hall current sensor.

Features

- 5V power supply
- On-board power indicator
- Bidirectional current measurement up to 5A
- Analog output with a sensitivity of 185 mV / A[40].

4.4 Voltage divider

When utilizing the common 5V analog reference voltage, the Arduino's analog inputs can measure DC voltage between 0 and 5V; this range can be expanded by using two resistors to make a voltage divider. The voltage divider brings the observed voltage down to a level compatible with the Arduino analog inputs[41].

4.5 LCD 16×2

LCD is an abbreviation for liquid crystal display. It is a type of electronic display module that is utilized in a wide range of applications such as various circuits and devices such as mobile phones, calculators, computers, and television sets. LCD is an abbreviation for liquid

crystal display. It is a type of electronic display module that is utilized in a wide range of applications such as various circuits and devices such as mobile phones, calculators, computers, and television sets.

The 4.3 shows the LCD 16*2.

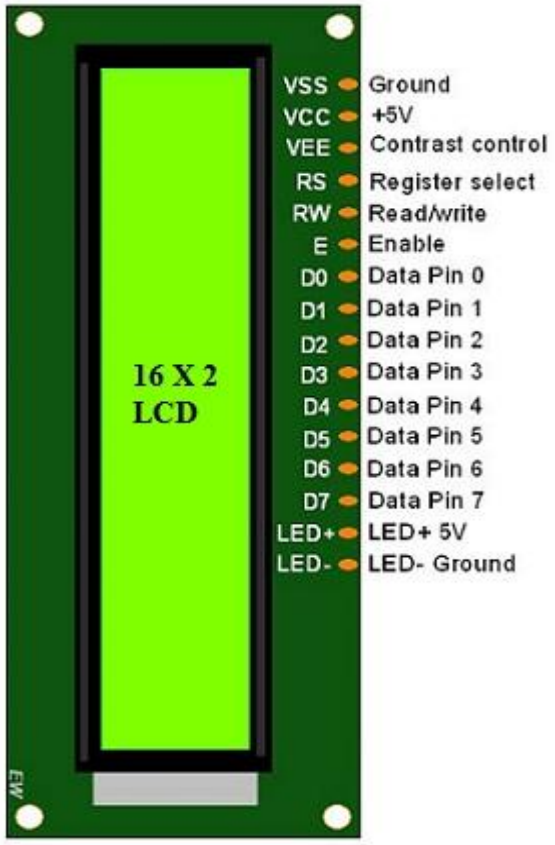

Figure4.3 : LCD 16×2.

4.5.1 Registers of LCD

A 16×2 LCD contains two registers, one for data and one for commands. The RS (register select) is mostly used to switch between registers. It is known as a command register when the register set is '0'. Similarly, when the register set is '1', it is referred to as a data register.

1. **Command Register**

The command register's primary role is to store command instructions sent to the display. So that predetermined actions like cleaning the display, initializing, setting the cursor position, and controlling the display can be performed. Within the register, commands can be processed.

2. Data Register

The data register's primary role is to store the information that will be displayed on the LCD panel. The ASCII value of the character is the information that will be displayed on the LCD screen. When we give information to the LCD, it sends to the data register, and the process begins there. When register set =1, the data register is chosen[42].

4.6 Realization of boost converter and implementation of MPPT.

The figure 4.5 and 4.6 below represents the diagram of the PCB of the boost converter designed in proteus.

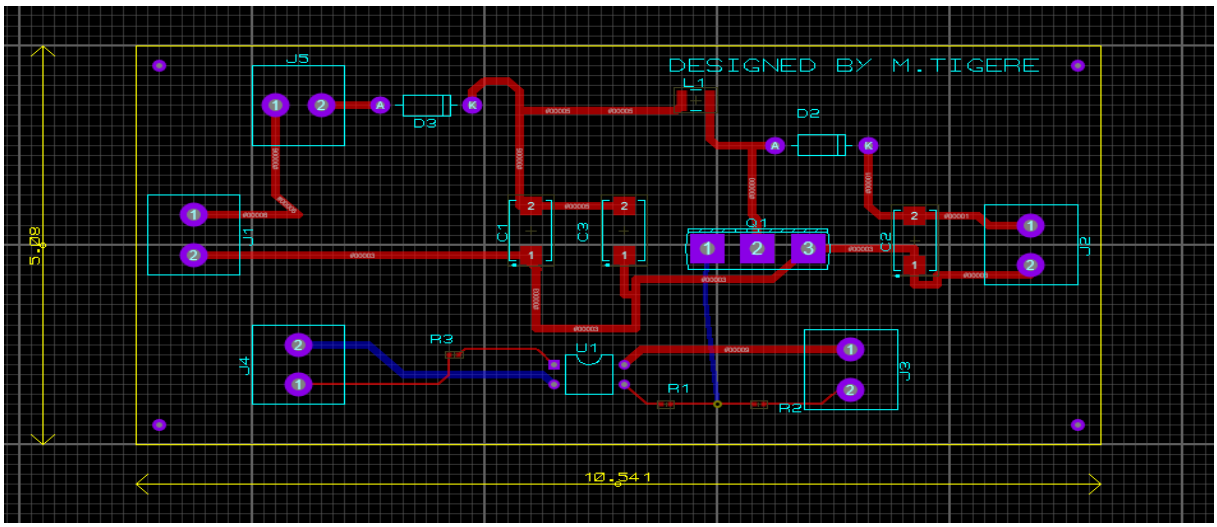

Figure4.4: The PCB of boost converter in 2D dimension.

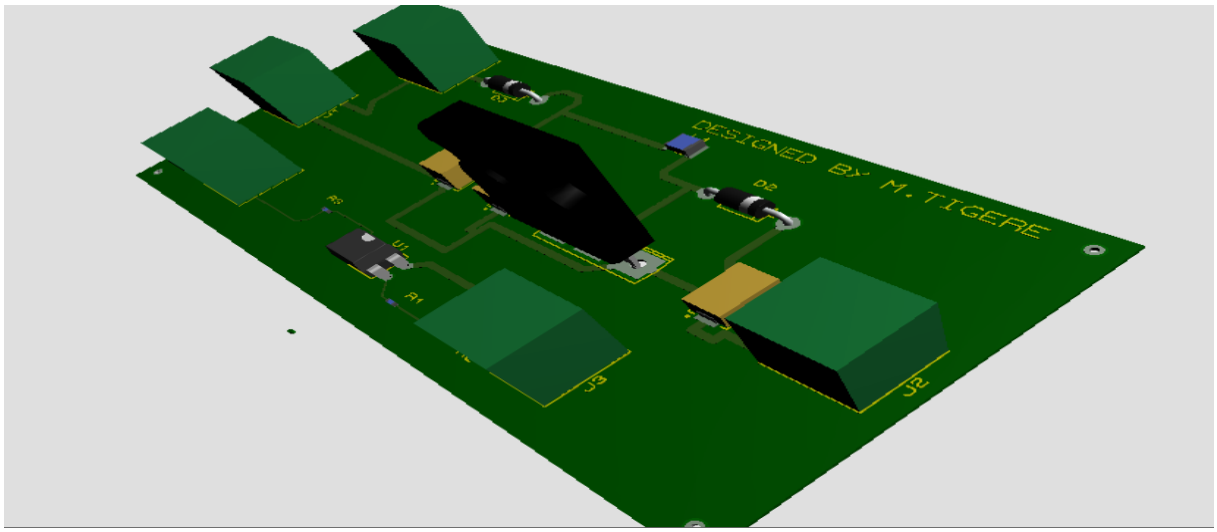

Figure4.5: The PCB of boost converter in 3D dimension.

f_s=25KHz

V_{mpw}=0.9*V_{mp} (4.1)

P_{mpw}=0.05*P_{mp} (4.2)

I_{mpw}=$\frac{P_{mpw}}{V_{mpw}}$ (4.3)

△V=2% (4.4)

△I=40% (4.5)

R_{mp} and R_{mpw}

$R_o = 2.5 * R_{mpw}$ (4.6)

$D_{mp(w)} = 1 - \sqrt{\frac{R_{mp(w)}}{R_o}}$ (4.7)

$V_{o(w)} = \frac{V_{mp(w)}}{1-D_{mp(w)}}$ (4.8)

$I_{o(w)} = \frac{V_{0(w)}}{R_0}$ (4.9)

$R_i = R_0(1 - D^2)$ only for 1000W/m^2 (4.10)

$C_i \geq \frac{4\, V_{mp} D_{mp}}{\triangle V_i R_i f_s}$ only for 1000W/m^2 (4.11)

$C_o \geq \frac{2\, D_{mp}}{\triangle V_o R_o f_s}$ only for 1000W/m^2 (4.12)

L$\geq \frac{V_{mp} D_{mp}}{2 \triangle I_o f_s}$ only for 50W/m^2 (4.13)

Implementation values in boost converter: (L=220µH,C_i=2000µF,$C_o = 100 \mu F$).

The figure 4.6 below shows the 3.8W solar panel

Figure 4.6: The solar panel used in the implementation of MPPT.

The table below shows the parameters of a 3.8W solar panel

Table 4.1: parameters of a solar panel.

Maximum Power (P_{max})	3.8W
Voltage at P_{max}	6V
Current at P_{max}	0.63A
Open Circuit Voltage (V_{oc})	7.2V
Short Circuit Current (I_{sc})	0.638A
Power Tolerance	±3%
Measurement	254*140*15MM

The figure 4.7 below shows PWM signal from the Arduino.

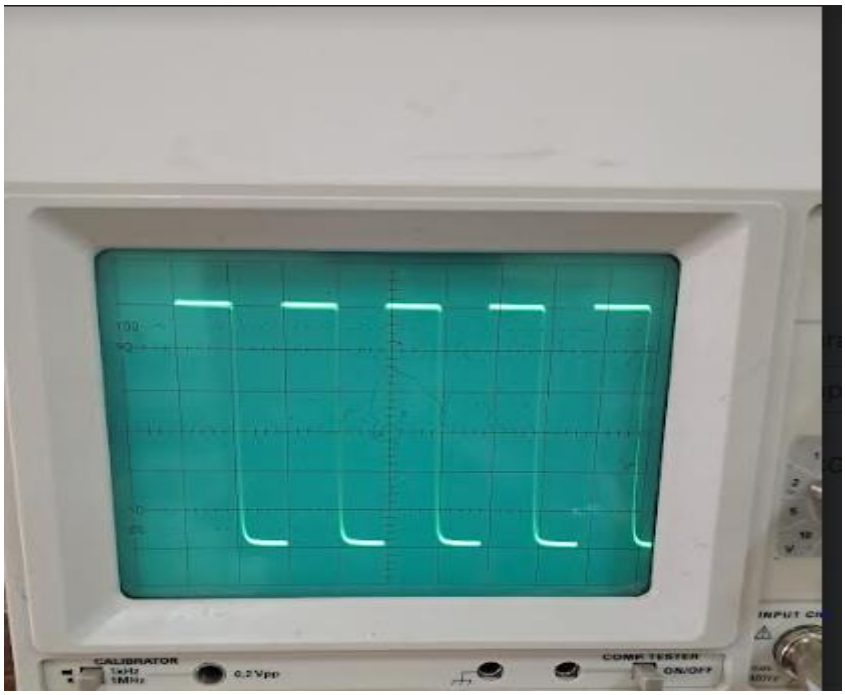

Figure 4.7: Implementation pwm signal on oscilloscope

The figure 4.8 below represents the complete diagram for the implementation of MPPT.

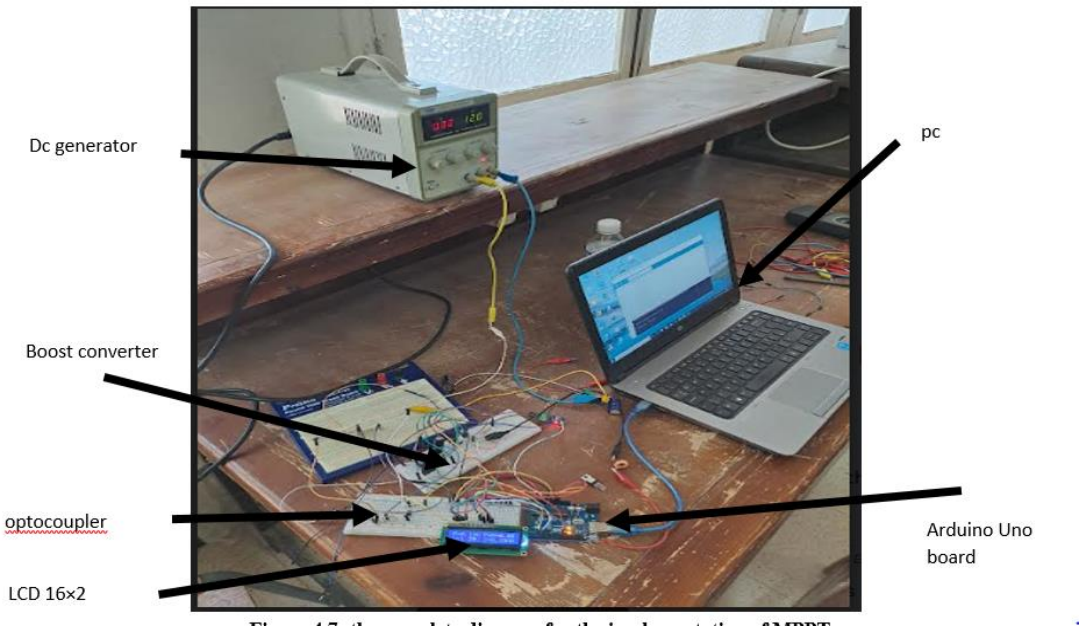

Figure 4.8: The complete diagram for the implementation of MPPT.

4.7 Test results

In this realization, I did tests with the P&O method at different hours of the day for maximum irradiance at that time and for the case where there is complete shading on the surface of the solar panel. I put the solar panel under the tree for the case where there is shading. This graphs were taken using Arduino graph plotter.

4.7.1 P&O method

The figures below shows the graphs of Power(W) in function of time(s) for different times of the day under sunlight and under shading.

- **At 9:30**

a) Solar panel in sunlight

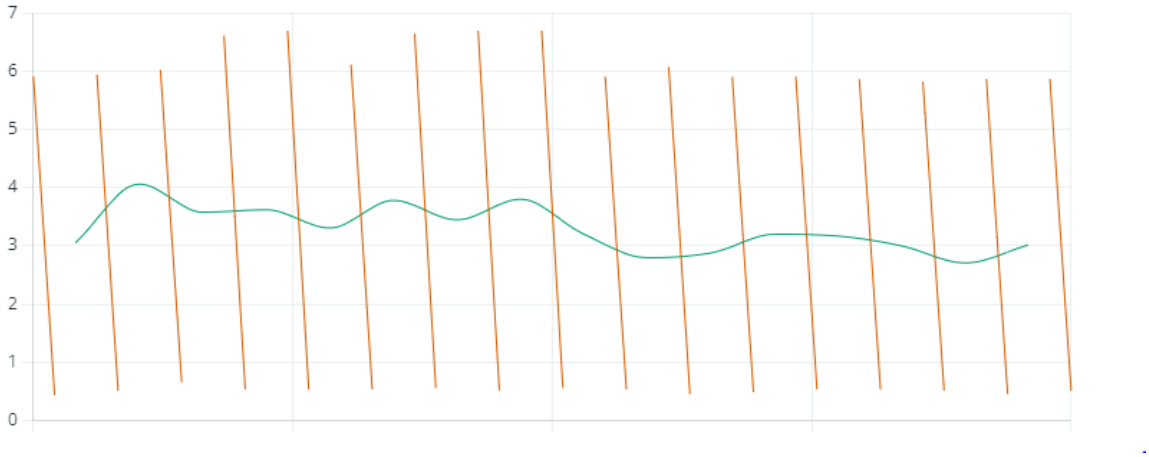

Figure4.9: solar panel power at 9:30 in sunlight.

The power was oscillating around 3.6Watts then it dropped to 3Watts.

b) solar panel under shading

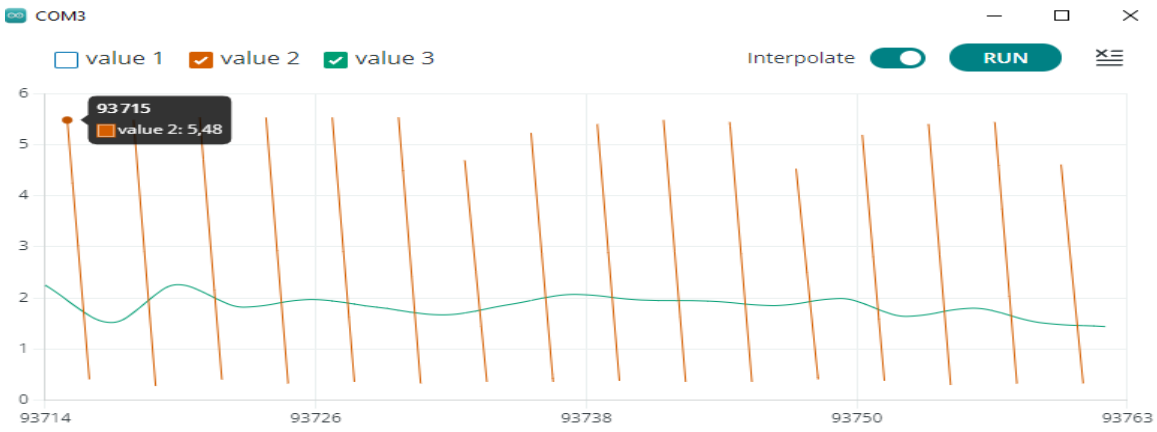

Figure4.10: solar panel power at 9:30 under shading effect.

The power was oscillating around 2Watts under shading.

- **At 10:30**

a) Solar panel in sunlight

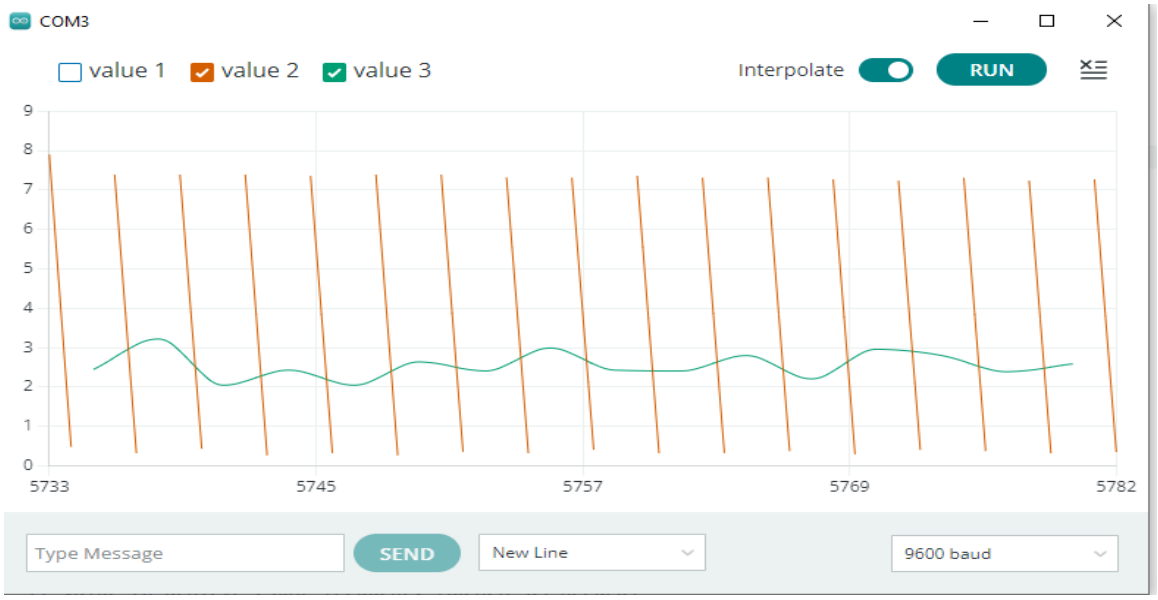

Figure4.11: solar panel power at 10:30 in sunlight.

The power was oscillating around 2.5Watts under sunlight at 10:30.

b) Under shading

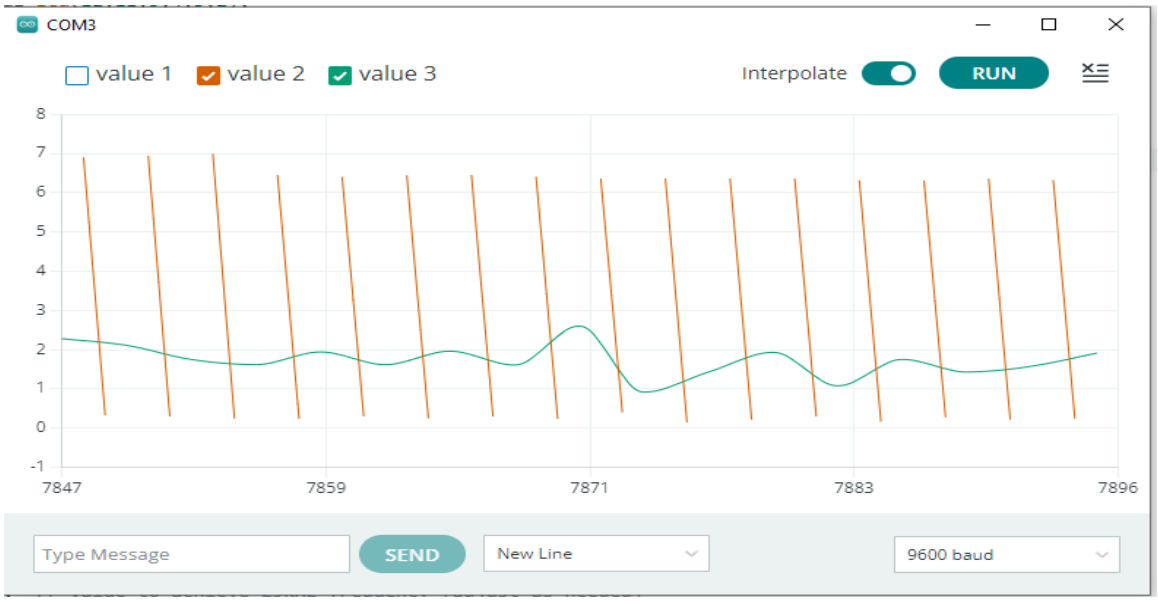

Figure4.12: solar panel power at 10:30 under shading effect.

The power was oscillating around 2Watts then it dropped to 1.5Watts under shading effect.

- **At 11:30**

a) Solar panel in sunlight

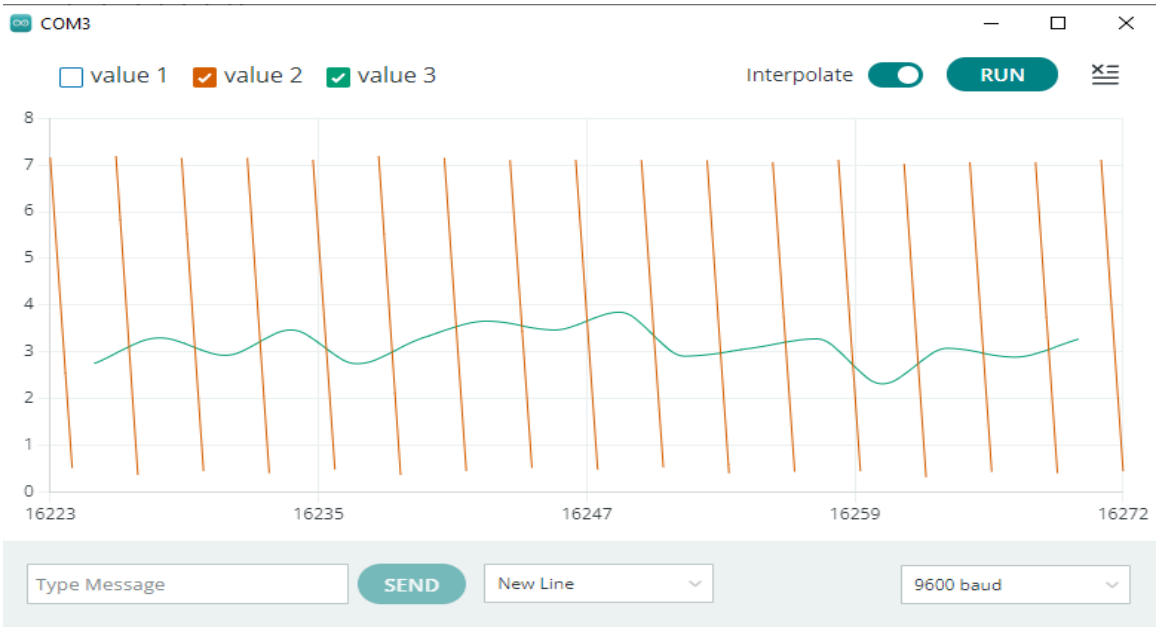

Figure4.13: solar panel power at 11:30 in sunlight.

The power was oscillating around 3.2Watts then it dropped to 3Watts.

b) Under shading

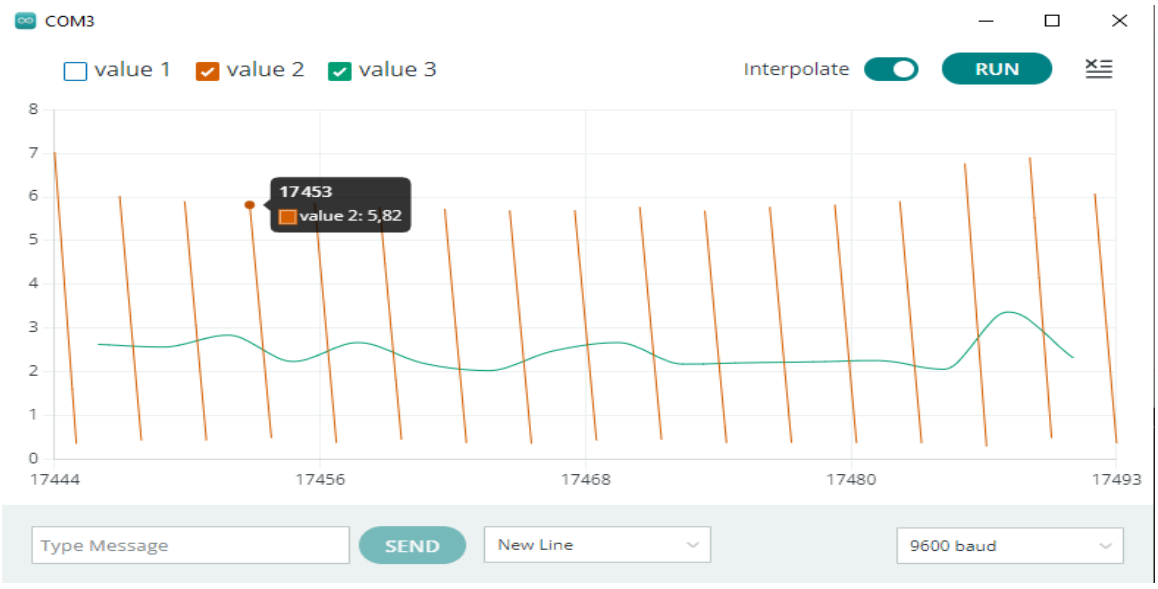

Figure4.14: solar panel power at 11:30 under shading effect.

The power was oscillating around 2.5Watts snd 2.2 Watts.

- **At 12:30**

a)Solar panel in sunlight

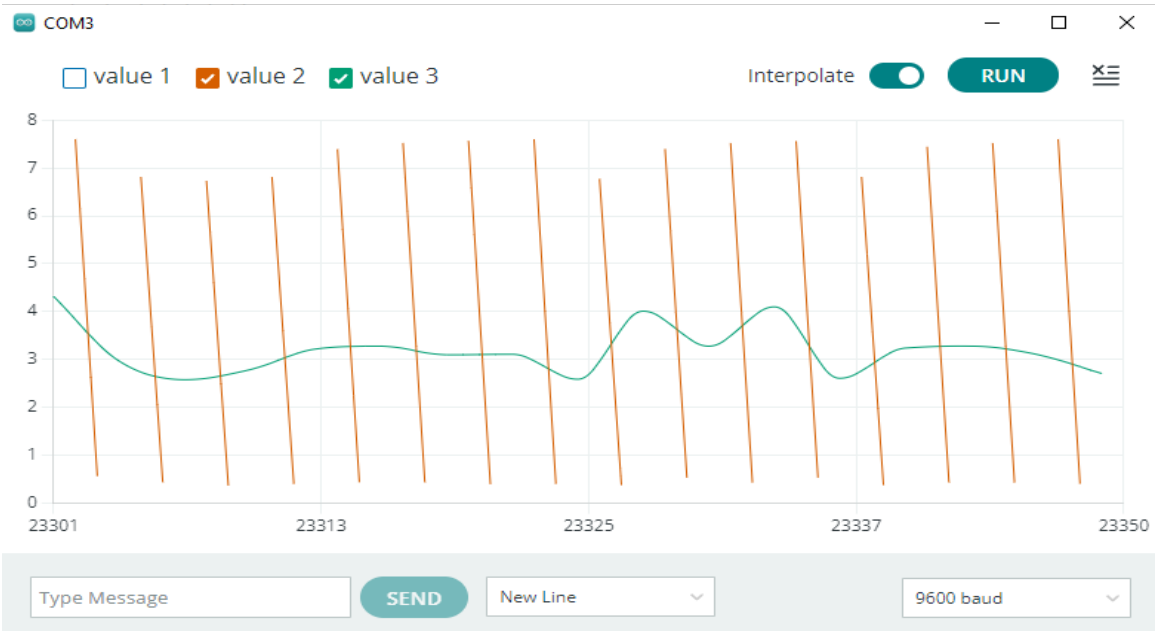

Figure4.15: solar panel power at 12:30 in sunlight.

The power was oscillating around 3Watts then it increased to 3.5Watts.

b) Under shading

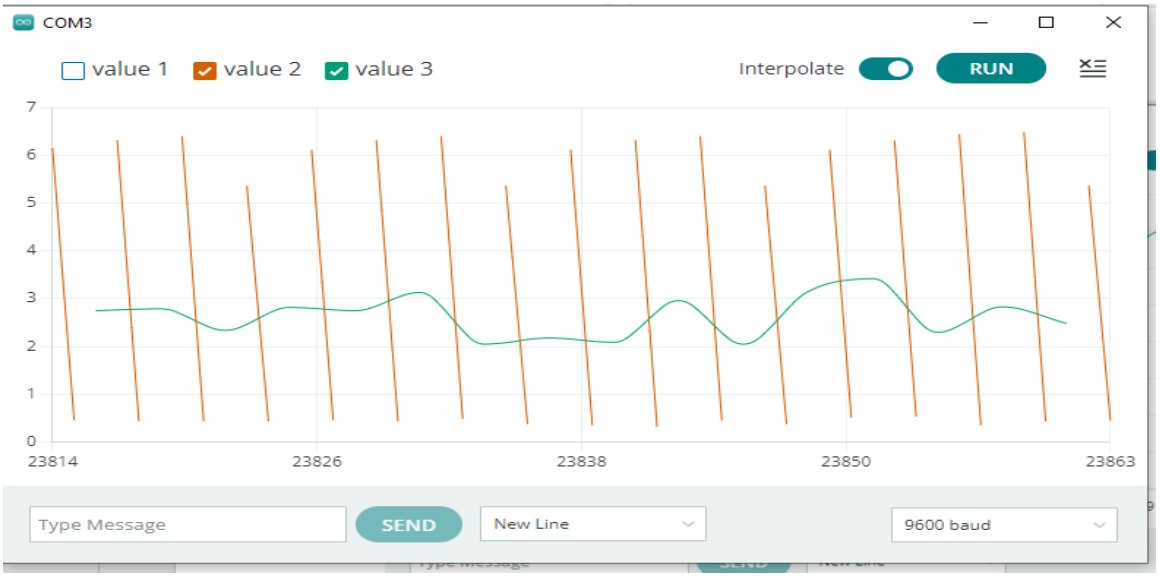

Figure4.16: panel power at 12:30 under shading effect.

The power was oscillating around 2.8Watts.

- **At 13:30**

a) Solar panel in sunlight

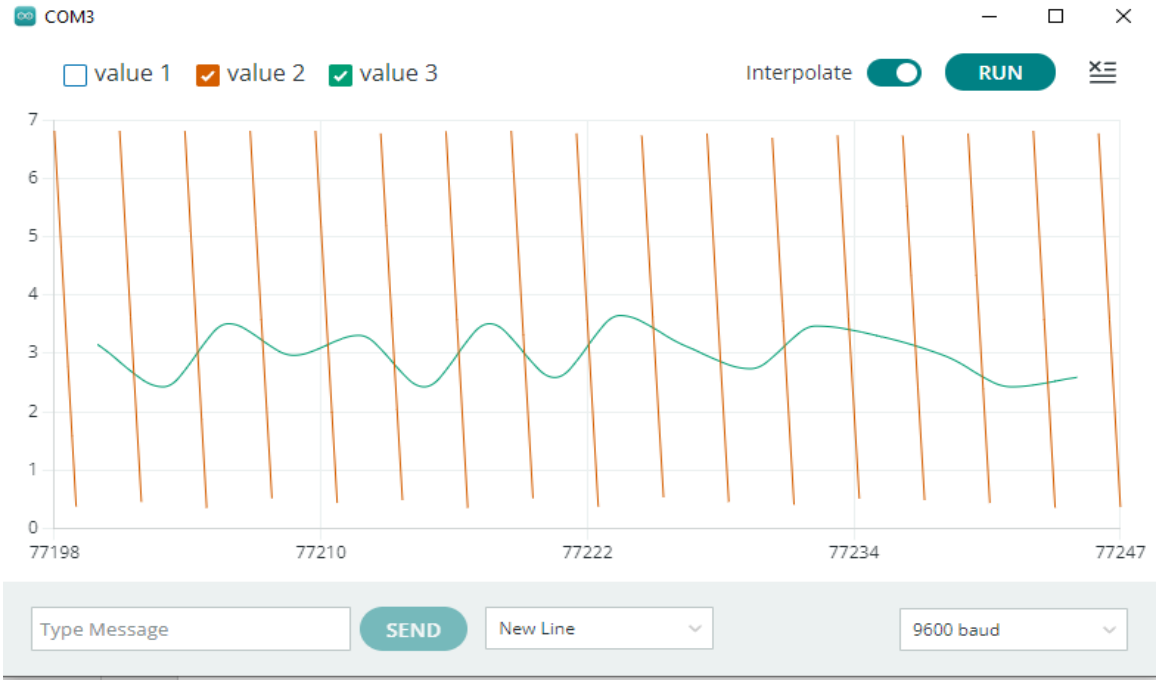

Figure4.17: solar panel power at 13:30 in sunlight.

The power was oscillating around 3Watts under sunlight.

b) Under shading

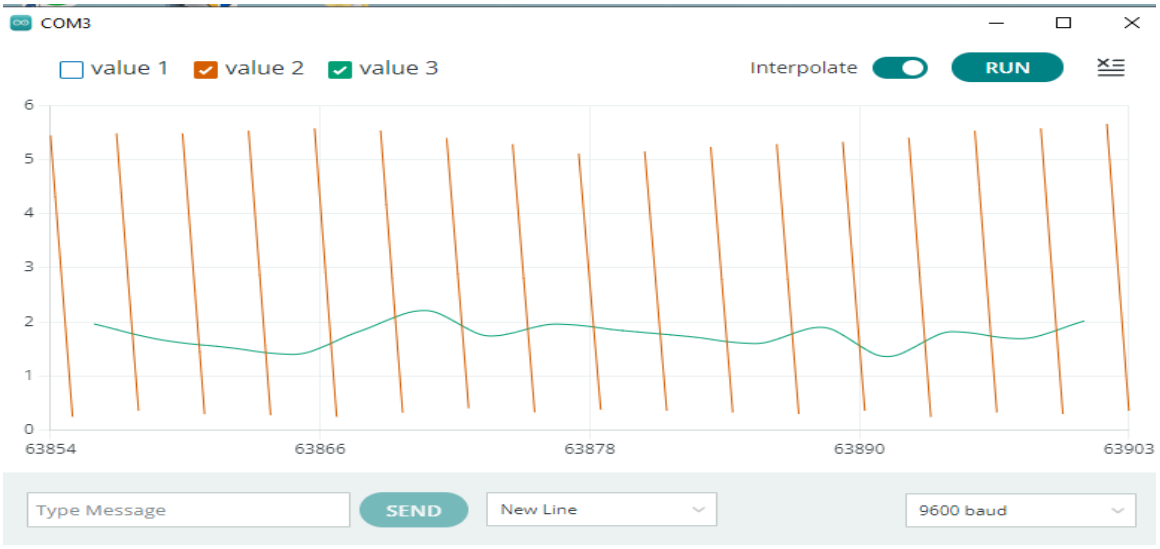

Figure 4.18: solar panel power at 13:30 under shading effect.

The power was oscillating around 2Watts.

- **At 14:30**

a) Solar panel in sunlight

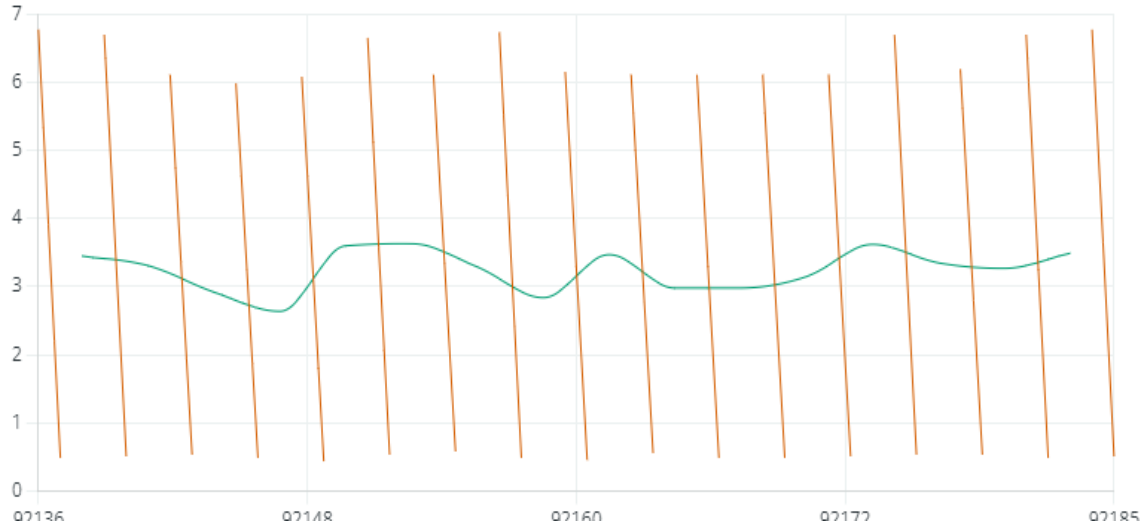

Figure4.19: solar panel power at 14:30 in sunlight.

The power was oscillating around 3.6W.

b) Under shading

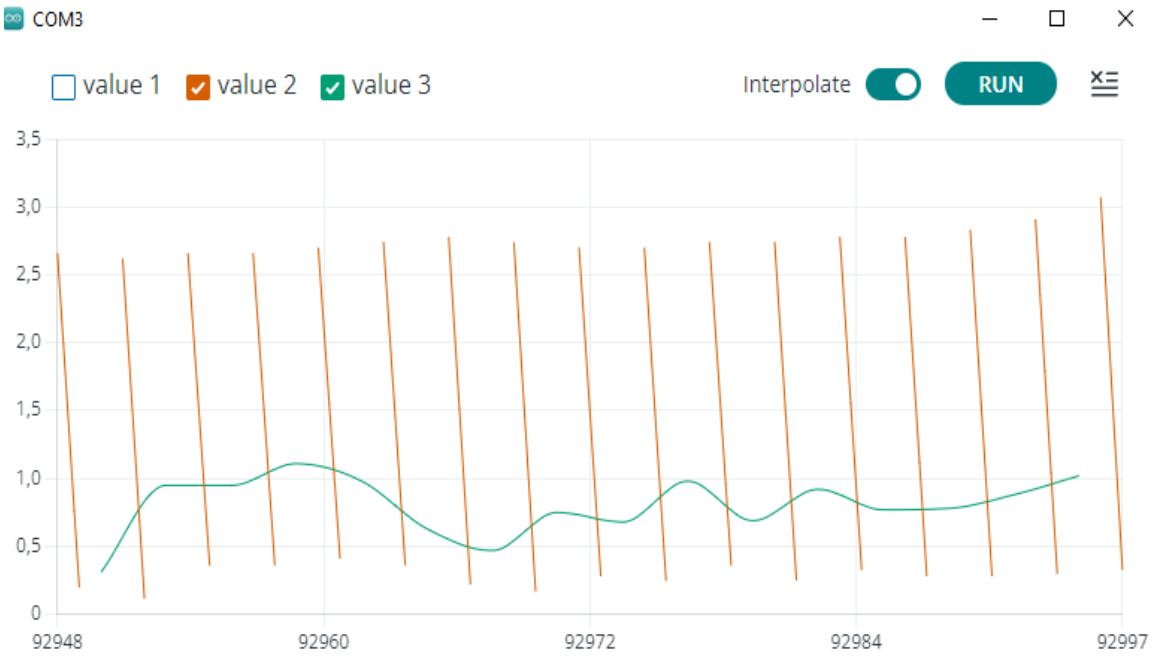

Figure 4.20: solar panel power at 14:30 under shading effect.

The power was oscillating around 1Watts and 1.5Watts.

4.8 Interpretation of results

The P&O method is generally effective in tracking and maintaining the solar panel's operation near its maximum power point. Under rapid changing conditions, it may not always be efficiency. One common issue with P&O method is oscillations around the maximum power point. The algorithm may cause the operating point to overshoot or undershoot the optimal point, resulting in power fluctuations. These oscillations can impact system stability and introduce inefficiencies. The results can be impacted by the quality of hardware and sensor accuracy. We have observed that the power being produced by solar panel is low under the conditions where there is shading. The irradiance reaching the solar panel reduces due to reduced number of photons reaching the surface of the solar panel under shading. The duty cycle of the Dc Dc boost converter is approximately 0.06.

4.9 conclusion

The practical tests on a solar panel by programming an Arduino Uno board. From these tests we have concluded that the boost converter can draw the maximum power from the PV generator by adjusting the duty cycle. We have observed that the power produced by a solar panel when placed in places where there is no shading is higher as compared to a solar panel under shading conditions. The boost converter supplies a voltage at its output higher than that provided by a PV panel. The P&O algorithm can be sensitive to noise and measurement errors in the voltage and current measurements used for tracking the MPP. These inaccuracies can affect the algorithm's performance and introduce deviations from the true MPP.

General Conclusion

This dissertation concerns the study and realization of a PV system adapted by an MPPT control ensuring the continuation of the maximum power supplied by the solar panel.

MPPT algorithms continuously monitor the PV solar panel voltage, current and power characteristics to adjust the operating point. Real time tracking allows the system to respond to rapid environment changes and maintain optimal power output, maximizing energy production. Selecting an appropriate MPPT algorithm and optimizing its parameters are essential for achieving optimal power output and maximizing the return on investment in PV installations.

In this dissertation we simulated the PV system adapted by P&O algorithm under standard state conditions and under variable irradiance, we have noticed that the output characteristics of the system are affected by the boost converter. The components of a boost converter have to be calculated and tried in simulation before implementation of the system. The values of capacitors and Inductor are very important when implementing MPPT. The diode and Mosfet should support the maximum current of the solar panel.

After the simulation we made up boost converter which will step up the voltage across the charge. The diodes used in this implementation are IN4007 due to their fast switching frequency. One IN4007 diode is placed between the solar panel and the boost converter to prevent current from flowing backwards which might damage the solar panel. The IRFP250N is used due to its heat resistant as compared to other Mosfets. We have used the LCD to display the power, current and voltage produced from the solar panel. The ACS 712 (0.5B) current sensor is used to measure the analogue values of current and sends the information to the Arduino UNO in digital form. The voltage divider is used to reduce the voltage of the solar panel to a level compatible with the microcontroller(5V). The algorithm will then calculate the power from voltage and current values then compares it to the previous power. The Arduino UNO provider the pwm signal from pin 6, for switching of the mosfet we put the optocoupler pc 817 between pin 6 of Arduino and mosfet. The pin 4 of optocoupler is connected to 12V which is needed to turn on the mosfet. The frequency used in this implementation is 25KHz.

The problems faced in this implementation are:

1)The ACS 712 current sensor is not accurate when the values of current being measured are small.

2)there is already current flowing in the LCD before connecting it to the solar panel, this current is the one used to turn on the background light of the LCD.

Improvements which can be made:

1) Use of high accurate current and voltage sensors.
2) Use of other microcontrollers with large memories.

Bibliography

[1] Tyagi VV, Rahim NAA, Rahim NA, et al. Progress in solar PV technology: Research and achievement. *Renew Sustain Energy Rev* 2013; 20: 443–461.

[2] Elyaqouti M, Hakim S, Farhat S, et al. Implementation in Arduino of MPPT using variable step size P&O algorithm in PV installations. *Int J Power Electron Drive Syst* 2017; 8: 434.

[3] Ali R. *Effect of Solar Panel Cooling on Photovoltaic Performance*. ProQuest Dissertations Publishing, https://www.proquest.com/docview/1560875816/330D3E1C747F46B4PQ/9 (2014, accessed 27 March 2023).

[4] Kumar NM, Subathra MSP, Moses JE. On-Grid Solar Photovoltaic System: Components, Design Considerations, and Case Study. In: *2018 4th International Conference on Electrical Energy Systems (ICEES)*. Chennai: IEEE, pp. 616–619.

[5] Vidyanandan KV. An Overview of Factors Affecting the Performance of Solar PV Systems. *Energy Scan House J Corp Plan NTPC Ltd* 2017; 27: 2–8.

[6] Chikate BV, Sadawarte Y, Sewagram B. The factors affecting the performance of solar cell. *Int J Comput Appl* 2015; 1: 0975–8887.

[7] Hurter WS, du Plessis H, van Rensburg NJ. Simplified encapsulation of solar cells using glass fibre reinforced polymers. In: *2013 Africon*. 2013, pp. 1–5.

[8] Wirth H, Weiß K-A, Wiesmeier C. Photovoltaic Modules: Technology and Reliability. In: *Photovoltaic Modules*. De Gruyter. Epub ahead of print 12 September 2016. DOI: 10.1515/9783110348286.

[9] Osigwe C. *Thévenin Equivalent of Solar Cell Model*. ProQuest Dissertations Publishing, https://www.proquest.com/docview/2379534165/47772426EEB24D89PQ/3 (2019, accessed 28 March 2023).

[10] Wani C 1, Gupta KK 1 1 SNMPS of TM, Engineering S-425405 (M S). Towards improving the performance of solar photovoltaic energy system: A review. Epub ahead of print February 2019. DOI: 10.1088/1755-1315/227/2/022009.

[11] Furkan D, Mehmet Emin M. Critical Factors that Affecting Efficiency of Solar Cells. *Smart Grid Renew Energy*; 2010. Epub ahead of print 31 May 2010. DOI: 10.4236/sgre.2010.11007.

[12] Elsaidi A. *Photovoltaic (PV) type solar generators and their effect on distribution systems*. ProQuest Dissertations Publishing, https://www.proquest.com/docview/1441075481/DFCBA1016E444110PQ/1 (2013, accessed 28 March 2023).

[13] Hybrid Solar System: Working, Price, Types, Pros, and Cons. *Solar Square Blog*, https://www.solarsquare.in/blog/hybrid-solar-inverter/ (2022, accessed 28 March 2023).

[14] Mrabti T, El Ouariachi M, Tidhaf B, et al. Regulation of electric power of photovoltaic generators with DC-DC converter (buck type) and MPPT command. In: *2009 International Conference on Multimedia Computing and Systems*. Ouarzazate, Morocco: IEEE, pp. 322–326.

[15] M. Biswal, 'Control Techniques for DC-DC Buck Converter with Improved Performance', Master Thesis, National Institute of Technology, Rourkela, March 2011. - Google Search, https://www.google.com/search?q=M.+Biswal%2C+%22Control+Techniques+for+DC-DC+Buck+Converter+with+Improved+Performance%22%2C+Master+Thesis%2C+National+Institute+of+Technology%2C+Rourkela%2C+March+2011.&oq=M.+Biswal%2C+%22Control+Techniques+for+DC-DC+Buck+Converter+with+Improved+Performance%22%2C+Master+Thesis%2C+National+Institute+of+Technology%2C+Rourkela%2C+March+2011.&aqs=chrome..69i57.1112j0j15&sourceid=chrome&ie=UTF-8 (accessed 28 March 2023).

[16] Sturm GD. *Single Sensor Maximum Power Point Tracking Algorithm for Photovoltaic Applications*. ProQuest Dissertations Publishing, https://www.proquest.com/docview/2070530654/28FAB9BBF154F21PQ/2 (2017, accessed 28 March 2023).

[17] Al-Gizi AG. Comparative study of MPPT algorithms under variable resistive load. In: *2016 International Conference on Applied and Theoretical Electricity (ICATE)*. Craiova, Romania: IEEE, pp. 1–6.

[18] Boost converter PDF - Google Search, https://www.google.com/search?sxsrf=APwXEdd4UoX0e4uG39N3F6fi7577w0PoPQ:1680056543959&q=Boost+converter+PDF&sa=X&ved=2ahUKEwjChIWsioD-AhWciv0HHTuHChkQ1QJ6BAhQEAE&biw=1366&bih=600&dpr=1 (accessed 29 March 2023).

[19] Patel DR. *Design of boost converter and resonant inverter for Jacob's ladder electric arc generation*. ProQuest Dissertations Publishing, https://www.proquest.com/docview/1418033072/706BD697DFC24143PQ/1 (2013, accessed 29 March 2023).

[20] Boost Switching Converter Design Equations, https://www.daycounter.com/LabBook/BoostConverter/Boost-Converter-Equations.phtml (accessed 29 March 2023).

[21] Bifurcation behavior of the buck converter, https://ieeexplore.ieee.org/abstract/document/491637/ (accessed 29 March 2023).

[22] What is a Buck Converter? *CircuitBread*, https://www.circuitbread.com/ee-faq/what-is-a-buck-converter (2020, accessed 29 March 2023).

[23] Etude et réalisation d'un chargeur solaire par Arduino - Google Search, https://www.google.com/search?q=Etude+et+r%C3%A9alisation+d%E2%80%99un+chargeur+solaire+par+Arduino&oq=Etude+et+r%C3%A9alisation+d%E2%80%99un+chargeur+solaire++par+Arduino&aqs=chrome..69i57.9002j0j15&sourceid=chrome&ie=UTF-8 (accessed 29 March 2023).

[24] design of an arduino based maximum power point tracking - Google Search, https://www.google.com/search?q=design+of+an+arduino+based+maximum+power+point+tracking&oq=design+of+an+arduino+based+maximum+power+point+tracking&aqs=chrome..69i57j33i160l2.45800j0j15&sourceid=chrome&ie=UTF-8 (accessed 30 March 2023).

[25] Guldemir H. Modeling and sliding mode control of dc-dc buck-boost converter. In: *Proc. 6th Int. advanced technological Symp*. 2011, pp. 475–480.

[26] Jain K, Gupta M, Kumar Bohre A. Implementation and Comparative Analysis of P&O and INC MPPT Method for PV System. In: *2018 8th IEEE India International Conference on Power Electronics (IICPE)*. JAIPUR, India: IEEE, pp. 1–6.

[27] Noguchi T, Togashi S, Nakamoto R. Short-current pulse-based maximum-power-point tracking method for multiple photovoltaic-and-converter module system. *IEEE Trans Ind Electron* 2002; 49: 217–223.

[28] Bhatnagar P, Nema RK. Maximum power point tracking control techniques: State-of-the-art in photovoltaic applications. *Renew Sustain Energy Rev* 2013; 23: 224–241.

[29] Podder AK, Roy NK, Pota HR. MPPT methods for solar PV systems: a critical review based on tracking nature. *IET Renew Power Gener* 2019; 13: 1615–1632.

[30] The physics and engineering of photovoltaic conversion, technologies and systems Arno HM Smets Klaus Jäger Olindo Isabella - Google Search, https://www.google.com/search?q=The+physics+and+engineering+of+photovoltaic+conversion%2C+technologies+and+systems+Arno+HM+Smets+Klaus+J%C3%A4ger+Olindo+Isabella&oq=The+physics+and+engineering+of+photovoltaic+conversion%2C+technologies+and+systems+Arno+HM+Smets+Klaus+J%C3%A4ger+Olindo+Isabella&aqs=chrome..69i57.8372j0j15&sourceid=chrome&ie=UTF-8 (accessed 8 April 2023).

[31] Chung HS-H, Tse KK, Hui SYR, et al. A novel maximum power point tracking technique for solar panels using a SEPIC or Cuk converter. *IEEE Trans Power Electron* 2003; 18: 717–724.

[32] D'Souza N, C. Lopes L, Liu X. Peak Current Control Based Maximum Power Point Trackers for Faster Transient Responses. In: *2006 Canadian Conference on Electrical and Computer Engineering*. Ottawa, ON, Canada: IEEE, pp. 659–663.

[33] Nissah Zainudin Hairul, Mekhilef Saad. Comparison study of maximum power point tracker techniques for PV systems. In: Proceedings of the 14th international middle east power systems conference (MEPCON'10), Cairo University, Egypt; December 19–21, 2010. Paper ID 278. - Google Search, https://www.google.com/search?q=Nissah+Zainudin+Hairul%2C+Mekhilef+Saad.+Co

mparison+study+of+maximum+power+point+tracker+techniques+for+PV+systems.+In%3A+Proceedings+of+the+14th+international+middle+east+power+systems+conference+(MEPCON%E2%80%9910)%2C+Cairo+University%2C+Egypt%3B+December+19%E2%80%9321%2C+2010.+Paper+ID+278.&oq=Nissah+Zainudin+Hairul%2C+Mekhilef+Saad.+Comparison+study+of+maximum+power+point+tracker+techniques+for+PV+systems.+In%3A+Proceedings+of+the+14th+international+middle+east+power+systems+conference+(MEPCON%E2%80%9910)%2C+Cairo+University%2C+Egypt%3B+December+19%E2%80%9321%2C+2010.+Paper+ID+278.&aqs=chrome..69i57.1589j0j15&sourceid=chrome&ie=UTF-8 (accessed 31 March 2023).

[34] Yaqoob SJ, Obed AA. Modeling, Simulation and Implementation of PV System by Proteus Based on Two-diode Model. *J Tech* 2019; 1: 39–51.

[35] Bellia H, Youcef R, Fatima M. A detailed modeling of photovoltaic module using MATLAB. *NRIAG J Astron Geophys*. Epub ahead of print 8 May 2019. DOI: 10.1016/j.nrjag.2014.04.001.

[36] Ideality Factor | PVEducation, https://www.pveducation.org/pvcdrom/solar-cell-operation/ideality-factor (accessed 8 April 2023).

[37] Ideality factor of various solar cells. *ResearchGate*, https://www.researchgate.net/figure/Ideality-factor-of-various-solar-cells_tbl1_357339559 (accessed 8 April 2023).

[38] commande MPPT de pas variable pour ameliorer les perfomance des systemes PV statiques et dynamiques - Google Search, https://www.google.com/search?q=commande+MPPT+de+pas+variable+pour+ameliorer+les+perfomance+des+systemes+PV+statiques+et+dynamiques&rlz=1C1SJWC_frDZ1053DZ1053&oq=commande+MPPT+de+pas+variable+pour+ameliorer+les+performance+des+systemes+PV+statiques+et+dynamiques&aqs=chrome..69i57.177329j0j15&sourceid=chrome&ie=UTF-8 (accessed 28 May 2023).

[39] Arduino UNO - JavaTpoint. *www.javatpoint.com*, https://www.javatpoint.com/arduino-uno (accessed 26 May 2023).

[40] ACS712 Hall Current Sensor (20A) | Open ImpulseOpen Impulse, https://www.openimpulse.com/blog/products-page/product-category/acs712-hall-current-sensor-20a/ (accessed 26 May 2023).

[41] Hareendran TK. DIY Arduino Voltmeter and Voltage Divider | ElectroSchematics. *ElectroSchematics.com*, https://www.electroschematics.com/arduino-digital-voltmeter/ (2013, accessed 26 May 2023).

[42] Agarwal T. LCD 16x2: Pin Configuration, Features and Its Working. *ElProCus - Electronic Projects for Engineering Students*, https://www.elprocus.com/lcd-16x2-pin-configuration-and-its-working/ (2019, accessed 27 May 2023).

Annexes

ACS712

Fully Integrated, Hall Effect-Based Linear Current Sensor with 2.1 kVRMS Voltage Isolation and a Low-Resistance Current Conductor

Features and Benefits

- Low-noise analog signal path
- Device bandwidth is set via the new FILTER pin
- 5 µs output rise time in response to step input current
- 80 kHz bandwidth
- Total output error 1.5% at T_A = 25°C
- Small footprint, low-profile SOIC8 package
- 1.2 mΩ internal conductor resistance
- 2.1 kV_{RMS} minimum isolation voltage from pins 1-4 to pins 5-8
- 5.0 V, single supply operation
- 66 to 185 mV/A output sensitivity
- Output voltage proportional to AC or DC currents
- Factory-trimmed for accuracy
- Extremely stable output offset voltage
- Nearly zero magnetic hysteresis
- Ratiometric output from supply voltage

TÜV America Certificate Number: U8V 06 05 54214 010

Package: 8 Lead SOIC (suffix LC)

Approximate Scale 1:1

Description

The Allegro® ACS712 provides economical and precise solutions for AC or DC current sensing in industrial, commercial, and communications systems. The device package allows for easy implementation by the customer. Typical applications include motor control, load detection and management, switched-mode power supplies, and overcurrent fault protection.

The device consists of a precise, low-offset, linear Hall sensor circuit with a copper conduction path located near the surface of the die. Applied current flowing through this copper conduction path generates a magnetic field which is sensed by the integrated Hall IC and converted into a proportional voltage. Device accuracy is optimized through the close proximity of the magnetic signal to the Hall transducer. A precise, proportional voltage is provided by the low-offset, chopper-stabilized BiCMOS Hall IC, which is programmed for accuracy after packaging.

The output of the device has a positive slope (>$V_{IOUT(Q)}$) when an increasing current flows through the primary copper conduction path (from pins 1 and 2, to pins 3 and 4), which is the path used for current sensing. The internal resistance of this conductive path is 1.2 mΩ typical, providing low power

Continued on the next page...

Typical Application

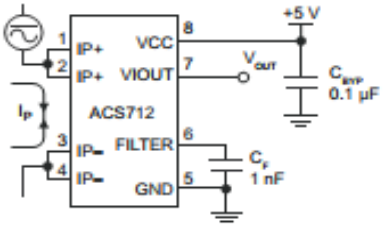

Application 1. The ACS712 outputs an analog signal, V_{OUT}, that varies linearly with the uni- or bi-directional AC or DC primary sensed current, I_P, within the range specified. C_F is recommended for noise management, with values that depend on the application.

Product Reference Manual
SKU: A000066

Description

The Arduino UNO R3 is the perfect board to get familiar with electronics and coding. This versatile microcontroller is equipped with the well-known ATmega328P and the ATMega 16U2 Processor.
This board will give you a great first experience within the world of Arduino.

Target areas:

Maker, introduction, industries

FAIRCHILD SEMICONDUCTOR®

IRF540N

Data Sheet **January 2002**

33A, 100V, 0.040 Ohm, N-Channel, Power MOSFET

Packaging

JEDEC TO-220AB

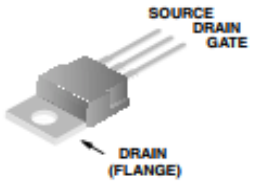

IRF540N

Features

- Ultra Low On-Resistance
  - $r_{DS(ON)}$ = 0.040Ω, V_{GS} = 10V
- Simulation Models
  - Temperature Compensated PSPICE™ and SABER© Electrical Models
  - Spice and SABER© Thermal Impedance Models
  - www.fairchildsemi.com
- Peak Current vs Pulse Width Curve
- UIS Rating Curve

Symbol

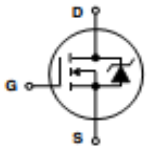

Ordering Information

PART NUMBER	PACKAGE	BRAND
IRF540N	TO-220AB	IRF540N

Absolute Maximum Ratings T_C = 25°C, Unless Otherwise Specified

		IRF540N	UNITS
Drain to Source Voltage (Note 1)	V_{DSS}	100	V
Drain to Gate Voltage (R_{GS} = 20kΩ) (Note 1)	V_{DGR}	100	V
Gate to Source Voltage	V_{GS}	±20	V
Drain Current			
Continuous (T_C = 25°C, V_{GS} = 10V) (Figure 2)	I_D	33	A
Continuous (T_C = 100°C, V_{GS} = 10V) (Figure 2)	I_D	23	A
Pulsed Drain Current	I_{DM}	Figure 4	
Pulsed Avalanche Rating	UIS	Figures 6, 14, 15	
Power Dissipation	P_D	120	W
Derate Above 25°C		0.80	W/°C
Operating and Storage Temperature	T_J, T_{STG}	-55 to 175	°C
Maximum Temperature for Soldering			
Leads at 0.063in (1.6mm) from Case for 10s	T_L	300	°C
Package Body for 10s, See Techbrief TB334	T_{pkg}	260	°C

NOTES:

1. T_J = 25°C to 150°C.

CAUTION: Stresses above those listed in "Absolute Maximum Ratings" may cause permanent damage to the device. This is a stress only rating and operation of the device at these or any other conditions above those indicated in the operational sections of this specification is not implied.

PC817 Series

High Density Mounting Type Photocoupler

● Lead forming type (I type) and taping reel type (P type) are also available. (PC817I/PC817P)
●● TÜV (VDE0884) approved type is also available as an option.

■ Features

1. Current transfer ratio
   (CTR: MIN. 50% at I_F = 5mA, V_{CE}=5V)
2. High isolation voltage between input and output (V_{iso}: 5 000V$_{rms}$)
3. Compact dual-in-line package
   PC817: 1-channel type
   PC827: 2-channel type
   PC837: 3-channel type
   PC847: 4-channel type
4. Recognized by UL, file No. E64380

■ Applications

1. Computer terminals
2. System appliances, measuring instruments
3. Registers, copiers, automatic vending machines
4. Electric home appliances, such as fan heaters, etc.
5. Signal transmission between circuits of different potentials and impedances

■ Outline Dimensions

(Unit: mm)

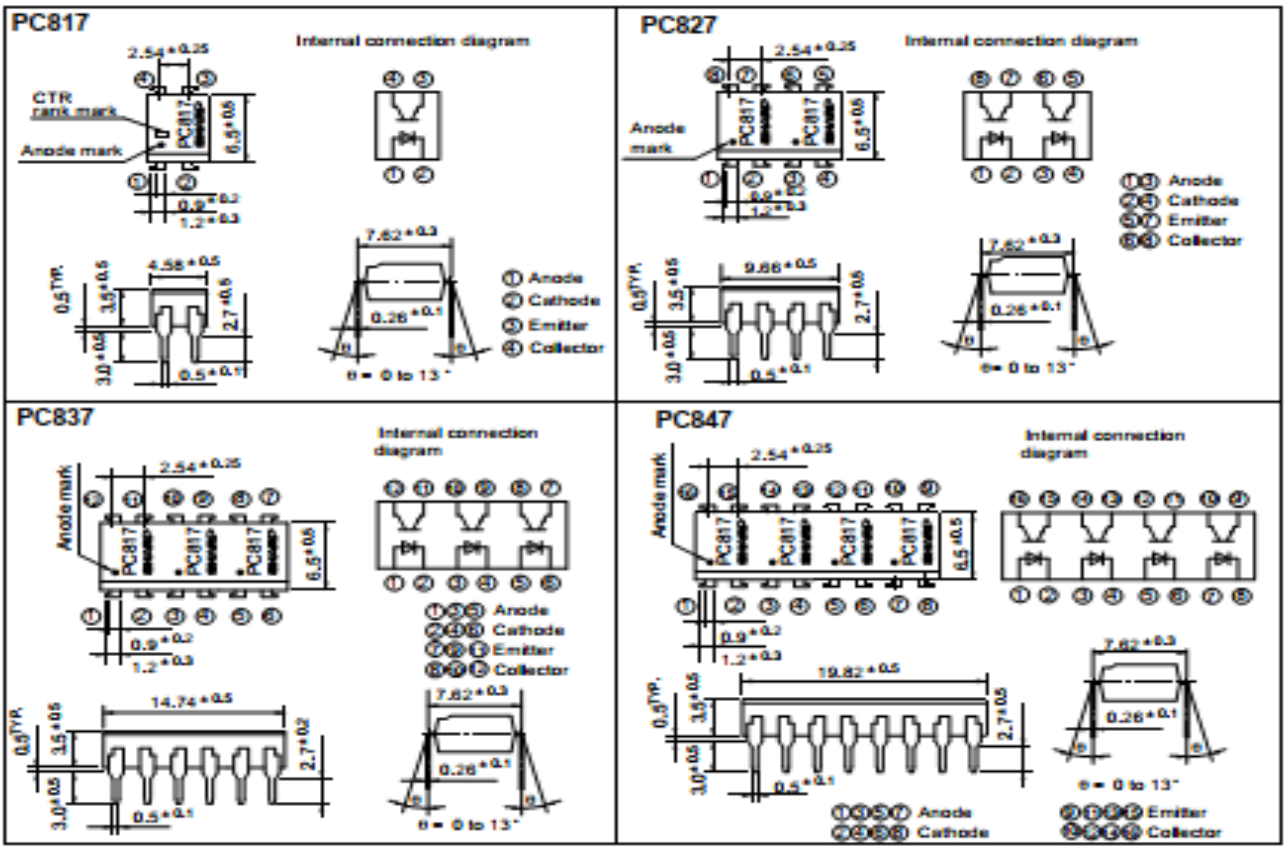

isc N-Channel MOSFET Transistor IRFP250N，IIRFP250N

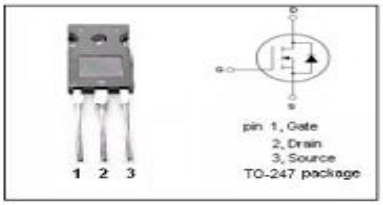

- **FEATURES**
- Static drain-source on-resistance:
  $R_{DS(on)} \leqslant 75m\Omega$
- Enhancement mode:
- 100% avalanche tested
- Minimum Lot-to-Lot variations for robust device performance and reliable operation

- **DESCRITION**
- Fast switching

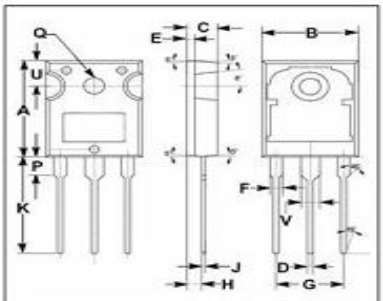

DIM	mm MIN	MAX
A	19.80	20.20
B	15.40	15.80
C	4.90	5.10
D	0.90	1.10
E	1.40	1.60
F	1.90	2.10
G	10.80	11.00
H	2.40	2.60
J	0.50	0.70
K	19.50	20.50
P	3.90	4.10
Q	3.30	3.50
U	5.20	5.40
V	2.90	3.10

- **ABSOLUTE MAXIMUM RATINGS(T_a=25℃)**

SYMBOL	PARAMETER	VALUE	UNIT
V_{DSS}	Drain-Source Voltage	200	V
V_{GS}	Gate-Source Voltage	±20	V
I_D	Drain Current-Continuous	30	A
I_{DM}	Drain Current-Single Pulsed	120	A
P_D	Total Dissipation @T_C=25℃	214	W
T_j	Max. Operating Junction Temperature	175	℃
T_{stg}	Storage Temperature	-55~175	℃

- **THERMAL CHARACTERISTICS**

SYMBOL	PARAMETER	MAX	UNIT
Rth(j-c)	Channel-to-case thermal resistance	0.7	℃/W
Rth(j-a)	Channel-to-ambient thermal resistance	40	℃/W